

International  
Progress Report

**IPR-99-17**

## Äspö Hard Rock Laboratory

Laboratory and field measurements  
of thermal properties of the rocks in  
the Prototype Repository at Äspö HRL

Jan Sundberg

Anna Gabrielsson

Swedish Geotechnical Institute

April 1999

***Svensk Kärnbränslehantering AB***

Swedish Nuclear Fuel

and Waste Management Co

Box 5864

SE-102 40 Stockholm Sweden

Tel 08-459 84 00

+46 8 459 84 00

Fax 08-661 57 19

+46 8 661 57 19



**Äspö Hard Rock  
Laboratory**

# Äspö Hard Rock Laboratory

## Laboratory and field measurements of thermal properties of the rocks in the Prototype Repository at Äspö HRL

Jan Sundberg

Anna Gabrielsson

Swedish Geotechnical Institute

April 1999

**Keywords:** Thermal properties, Mineral composition, Äspö

This report concerns a study which was conducted for SKB. The conclusions and viewpoints presented in the report are those of the author(s) and do not necessarily coincide with those of the client.



RAPPORTNUMMER

IPR-99-17

TILLHÖR/REG.NR

F63K

FÖRFATTARE

Jan Sundberg

Anna Gabrielsson

TILLSTYRKT

Lars-Olof Dahlström

Christer Svemar

GODKÄNT/FASTSTÄLLT

Olle Olsson

DATUM

April 99

DATUM

99-09-01

DATUM

99-09-03

# LABORATORY AND FIELD MEASUREMENTS OF THERMAL PROPERTIES OF THE ROCKS IN THE PROTOTYPE REPOSITORY AT ÄSPÖ HRL

Jan Sundberg  
Anna Gabrielsson  
Swedish Geotechnical Institute

April 1999

## Foreword

This report presents the result of an evaluation of thermal properties of the rock mass in the Prototype Repository tunnel at Äspö HRL. The evaluation is based on investigations of rock samples in the laboratory, thermal measurements in the laboratory and in the field, as well as calculations. The project was conducted by the Swedish Geotechnical Institute, on a commission by the Swedish Nuclear Fuel and Waste Management Co.

As a part of this work, samples of the rock were examined with respect to density and water absorption by the Swedish National Testing and Research Institute (SP). Geochemical and mineralogical composition of the rock were examined and evaluated by Terralogica AB. Laboratory measurements of thermal properties, at different levels of temperature, were performed by CIT Thermoflow AB. In the field, the measurements of thermal properties were carried out by the Swedish Geotechnical Institute.

## Abstract

Evaluations of thermal properties of the rock mass in the planned Prototype Repository at Äspö HRL have been performed based on measurements in the laboratory, in the field, and calculations.

The objective was to determine thermal properties of present rocks and the influence of anisotropies, so that the deposition hole distance or the power output can be designed and a valuation of planned long-term heating tests can be performed. The results will also serve as input data for the analysis of other thermally controlled processes. Finally, the project was to gain experience regarding the extent and accuracy of measurements required for forth-coming investigations of thermal properties for the localization of a deep repository.

Field measurements of thermal properties of the rock were performed in the tunnel for the planned Prototype Repository. The laboratory measurements of thermal properties were performed on samples from drill cores inside the tunnel. The rock samples were also investigated with respect to chemical and mineralogical composition, as well as density and porosity. Results from mineralogical analyses were used as input for calculations.

Based on assumptions of rock distribution, the thermal properties of the rock surrounding the Prototype Repository tunnel are estimated at:

Thermal conductivity	2.60 W/m°C
Thermal diffusivity	1.14 mm <sup>2</sup> /s
Heat capacity	2.22 MJ/m <sup>3</sup> °C

The values given above do not take into account effects on the thermal transport of large water-bearing fissures.

## Sammanfattning

En utvärdering av bergmassans termiska egenskaper i det planerade prototypförvaret vid Äspö HRL har gjorts baserat på resultat från mätningar i laboratorium, i fält och beräkningar.

Syftet med projektet var att bestämma de termiska egenskaperna för aktuella bergarter och inverkan av anisotropier så att dimensionerande kapselavstånd alternativt effektgenerering kan erhållas och en värdering av planerade långsiktiga uppvärmningsförsök kan utföras (prediktering–verifiering). Vidare skall projektet ge indata till andra temperaturstyrda processer. Slutligen syftade projektet till att vinna erfarenheter beträffande omfattning och noggrannhet av kommande undersökningar av termiska egenskaper vid lokalisering av djupförvar.

Mätningar av bergmassans termiska egenskaper utfördes inuti tunneln för det planerade prototypförvaret. Mätningar i laboratoriet av bergmassans egenskaper utfördes på bergprover från provtagning med kärnborr inuti tunneln. Bergproverna undersöktes också med avseende på kemisk och mineralogisk sammansättning samt densitet och porositet. Resultat från modalanalyser utgjorde indata till beräkningar.

Baserat på antagen bergartsfördelning bedöms bergmassan runt tunneln för det planerade prototypförvaret ha följande termiska egenskaper:

Värmekonduktivitet	2,60 W/m°C
Värmediffusivitet	1,14 mm <sup>2</sup> /s
Värmekapacitet	2,22 MJ/m <sup>3</sup> °C

De ovan givna värdena inkluderar inte påverkan på värmetransporten av större vattenförande sprickor.

## Executive Summary

Evaluations of thermal properties of the rock mass in the planned Prototype Repository at Äspö HRL have been performed based on measurements in the laboratory, in the field, and calculations.

The objective of the study was to determine thermal properties of present rocks and the influence of anisotropies, so that the deposition hole distance or the power output can be designed and an evaluation of planned long-term heating tests can be performed. The results will also serve as input data for the analysis of other thermally controlled processes. Finally, the project was to gain experience regarding the extent and accuracy of measurements required for forth-coming investigations of thermal properties for the localization of a deep repository.

The thermal properties of the rock surrounding the Prototype Repository tunnel is estimated at:

Thermal conductivity	2.60 W/m°C
Thermal diffusivity	1.14 mm <sup>2</sup> /s
Heat capacity	2.22 MJ/m <sup>3</sup> °C

The values of thermal properties are based on assumed distribution of different rocks. Based on drill cores, the surrounding rock consists of 96 % Äspö diorite and 4 % xenolith. The Äspö diorite is further subdivided in different groups with respect to the degree of alteration.

It should be noted that the values given above do not take into account effects on the thermal transport of large water-bearing fissures.

The dominating rock, Äspö diorite, shows various degrees of alteration with for some core samples a complete replacement of biotite by chlorite. This has a significant influence on the thermal properties, especially the thermal conductivity. The thermal conductivity of altered Äspö diorite, with high chlorite contents, is estimated at 2.70 W/m°C. The thermal conductivity of fresh Äspö diorite, with a significant amount of biotite still present, is estimated at 2.32 W/m°C.

Field measurements may be affected by heat convection caused by water flow within the rock and high water pressures inside the tunnel. Heat convection during measurements result in an overestimation of the thermal conductivity.

# Contents

<b>Foreword</b>	<b>i</b>
<b>Abstract</b>	<b>ii</b>
<b>Sammanfattning</b>	<b>iii</b>
<b>Executive Summary</b>	<b>iv</b>
<b>Contents</b>	<b>v</b>
<b>List of Figures</b>	<b>vii</b>
<b>List of Tables</b>	<b>viii</b>
<b>1 Introduction</b>	<b>1</b>
<b>2 Objectives</b>	<b>2</b>
<b>3 Geology in the Prototype Repository</b>	<b>3</b>
<b>4 Investigations</b>	<b>4</b>
<b>5 Description of Methods</b>	<b>6</b>
5.1 Laboratory Analyses of Density and Porosity	6
5.2 Analyses of Chemical and Mineralogical Composition	6
5.3 Laboratory Measurements of Thermal Properties	7
5.4 Field Measurements of Thermal Properties	8
5.5 Computer Calculations of Thermal Conductivity	11
<b>6 Density and Porosity</b>	<b>12</b>
<b>7 Mineral Composition</b>	<b>15</b>
<b>8 Thermal properties</b>	<b>18</b>
8.1 Results from Laboratory Measurements	18



8.2 Results from Field Measurements	21
8.3 Thermal Properties from Calculations	23
<b>9 Evaluation and Discussion</b>	<b>25</b>
9.1 Comparisons between Laboratory, Field and Calculated Results	25
9.2 Temperature Dependence of Thermal Properties	28
9.3 Comparisons with Previous Studies	29
9.4 Possible Reasons for Differences in the Results	31
<b>10 Conclusions</b>	<b>35</b>
<b>References</b>	<b>37</b>
<b>Appendix 1: Position of Field Measurements and Core Drillings for Laboratory Measurements</b>	<b>38</b>
<b>Appendix 2: Rock Classification of Drill Cores</b>	<b>40</b>
<b>Appendix 3: Density and Water Absorption of Core Samples</b>	<b>43</b>
<b>Appendix 4: Chemical Data of Core Samples</b>	<b>45</b>
<b>Appendix 5: Thermal Properties in the Laboratory</b>	<b>47</b>
<b>Appendix 6: Co-ordinates of Boreholes and Layout at the Thermal Probe Measurement Points</b>	<b>49</b>
<b>Appendix 7: Data and Graphic Presentations of the Results from Thermal Probe Measurements</b>	<b>53</b>

## List of Figures

Figure 5-1	Drilling of boreholes for thermal probe measurements in the tunnel for the Prototype Repository at Äspö.	9
Figure 5-2	Thermal probe measurements of thermal properties of the rocks in the tunnel for the Prototype Repository at Äspö.	10
Figure 5-3	Boreholes with installed probes at section 3522 inside the tunnel for the Prototype Repository. Installations in a dyke of mylonite. The heat generating probe is situated in the centre and two temperature probes at about 0.16 metres from the centre probe.	10
Figure 6-1	Density and water absorption of Äspö diorite and xenolith. Results from laboratory examinations of rock samples.	12
Figure 8-1	Thermal properties of rock samples. Results from measurements at temperature of 21 °C, with dry and saturated samples.	18
Figure 8-2	Thermal conductivity of Äspö diorite at different temperatures. From measurements in the laboratory.	19
Figure 8-3	Thermal diffusivity of Äspö diorite at different temperatures. From measurements in the laboratory.	20
Figure 8-4	Heat capacity of Äspö diorite obtained from measurements of thermal conductivity and thermal diffusivity in the laboratory.	20
Figure 9-1	Thermal conductivity of Äspö diorite from laboratory (21 °C, saturated conditions) and field measurements, and calculations based on mineral composition. Samples 3539-2 5.50-5.68, 3545 0.83-1.11 and 3551 0.95-1.15 represent altered Äspö diorite. Samples 3563 0.88-1.12, 3581 1.10-1.33 and 3587 0.97-1.14 represent fresh Äspö diorite.	25
Figure 9-2	Thermal diffusivity of Äspö diorite from laboratory (21 °C, saturated conditions) and field measurements.	26
Figure 9-3	Heat capacity of Äspö diorite based on measured values of thermal conductivity and thermal diffusivity in the laboratory (21 °C, saturated conditions) and in the field.	27
Figure 9-4	LOI content versus thermal conductivity measured in the laboratory (temperature 21 °C, saturated samples).	31

## List of Tables

Table 4-1	Samples for laboratory investigations. C = chemical analyses, D+P = density and porosity (water absorption) determinations and T = thermal conductivity measurements.	5
Table 6-1	Mean values and spreading intervals of the water absorption (volumetric %) before and after boiling the Äspö diorite samples in water for 5 hours, and with and without consideration of weight loss during water storage and boiling.	13
Table 6-2	Mean values and standard deviation of the density ( $\text{kg/m}^3$ ) for altered and fresh Äspö diorite and xenolith.	13
Table 6-3	Mean values of the water absorption (volumetric %) for altered and fresh Äspö diorite and xenolith. Before and after boiling, with and without consideration of weight loss during water storage and boiling. Standard deviations are written between brackets.	14
Table 7-1	Geochemical data of rock samples representing fresh Äspö diorite (ÄD) and altered Äspö diorite respectively.	15
Table 7-2	Mineralogical composition of rock samples representing fresh Äspö diorite (ÄD), altered Äspö diorite and xenolith, based on microscopy and chemical composition.	16
Table 8-1	Mean values of thermal properties and spreading intervals based on 10 rock samples of Äspö diorite. Results at a temperature of 21 °C, dry and saturated conditions.	19
Table 8-2	Thermal properties of the rocks measured with thermal probes. Values in brackets were obtained at conditions with high water flows.	22
Table 8-3	Calculated thermal conductivity of fresh Äspö diorite, altered Äspö diorite and xenolith. Results from Condrock calculations.	23
Table 8-4	Minerals found in samples of Äspö diorite (ÄD) and corresponding thermal conductivity used for the calculations (Sundberg 1988). Values in brackets are estimations.	23
Table 9-1	Thermal properties of Äspö diorite (ÄD). Mean values from measurements in the laboratory and in the field. Calculated thermal conductivity based average mineral compositions.	28

Table 9-2	Thermal properties measured in the field in three different sections in the tunnel for the Prototype Repository.	28
Table 9-3	Mean values of thermal conductivity and heat capacity at 25 °C, from calculations based on estimations of mineral composition of different rock types at Äspö (Sundberg, 1991).	30

# 1 Introduction

Important parts of the technique for storage of used nuclear fuel are developed and demonstrated at the Äspö Hard Rock Laboratory. Among many things, a prototype repository is under construction where criteria for canister placing, drilling technique, bentonite sealing and heat generation/spreading will be studied. The thermal development depends on the heat input, distance between the canisters and thermal properties of the surrounding media. For a certain maximum temperature of the canisters, the thermal properties of the rock mass are significant for the extension of the full-scale repository.

The Swedish Geotechnical Institute has been commissioned by the Swedish Nuclear Waste Management Co (SKB) to perform investigations of thermal properties of the rock mass in the Prototype Repository tunnel at Äspö.

## **2 Objectives**

The objective is to determine thermal properties of present rocks and the influence of anisotropies, so that the deposition hole distance or the power output can be designed and a valuation of planned long-term heating tests can be performed. The results will also serve as input data for the analysis of other thermally controlled processes. Finally, the project aims at gaining experience regarding the extent and accuracy of measurements required for forth-coming investigations of thermal properties for the localization of a deep repository.

### **3 Geology in the Prototype Repository**

The Prototype Repository tunnel at Äspö island is situated at the 450 meter level below the ground surface. The tunnel has a circular cross section, 5 metres in diameter. The length of the tunnel is about 90 metres.

The rock mass has been described for example by Patel et al (1997). According to this report the rock at the Prototype Repository consists of Äspö diorite with veins and inclusions of fine-grained granite. The main joint set trend WNW with steep dips. These joints are also the main water bearing structures. The total quantity of inflowing water into the prototype tunnel has been estimated at about 5 litres per minute.

## 4 Investigations

The investigations of the rock mass at the Prototype Repository tunnel comprised:

- Density and water absorption of rock samples.
- Modal analysis and chemical composition of rock samples.
- Laboratory measurements of thermal properties of rock samples.
- Field measurements of thermal properties.

Approximate positions for field measurements and core drillings along the Prototype Repository tunnel are shown in Appendix 1.

Samples were selected from existing drill cores evenly distributed along the prototype repository tunnel. At the time for sample selection 9 drill cores down to about 7 metres depth had been quality assured with respect to geological classification, see Appendix 2. Samples were taken at about 1 and 7 metres depth from each of these drill cores, in total 18 samples. 2 samples were taken from a middle level from two of the drill cores, at about 4 and 5 metres depth respectively. One of these samples was a xenolith. The other 19 samples consisted of Äspö diorite.

From each sample, individual samples were taken for either density and water absorption measurements, rock chemistry/mineralogical analyses or thermal properties measurements. This means that different samples were used for different types of investigations.

20 samples were examined with respect to rock chemistry. 11 samples were chosen for density and porosity (water absorption) examinations, microscopy/spectroscopy and thermal diffusivity and thermal conductivity measurements. Some additional determinations of density and water absorption were made using 4 of the samples.

Sample identification, depth and performed investigations are summarized in Table 4-1.

Laboratory measurements of thermal conductivity and thermal diffusivity were performed at 0 °C, at room temperature (21 °C) and at elevated temperatures, at the most at a temperature of 78 °C.

Field measurements of thermal conductivity and thermal diffusivity of the rock mass were performed at six locations inside the prototype tunnel at Äspö (3522, 3525, 3535, 3566, 3583 and 3594). The measurement depth was about 0.6 metres (from the floor of the tunnel). Results from the field measurements have previously been presented in report "Field measurements of thermal properties of the rocks in the prototype repository at Äspö HRL" (Sundberg & Gabrielsson, 1998).

The heat capacity of the rock mass was calculated using values of thermal diffusivity and thermal conductivity measured in the laboratory and in the field.



The Swedish National Testing and Research Institute (SP) performed laboratory examinations of rock samples with respect to density and water absorption. Geochemical and mineralogical composition of the rock were examined and evaluated by Terralogica AB. The laboratory measurements of thermal properties were performed by CIT Thermo-flow AB and in the field by the Swedish Geotechnical Institute.

**Table 4-1 Samples for laboratory investigations. C = chemical analyses, D+P = density and porosity (water absorption) determinations and T = thermal conductivity measurements.**

Identification	Depth (m)	Investigation
KA3539	1.0-1.22	C, D+P, T
	5.50-5.68	C, D+P, T
	7.0-7.17	C
KA3545	0.83-1.11	C, D+P, T
	6.99-7.10	C
KA3551	0.95-1.15	C, (D+P) <sup>*</sup> , T
	6.90-7.05	C
KA3563	0.88-1.12	C, D+P, T
	6.97-7.11	C
KA3569	0.87-1.20	C, (D+P) <sup>*</sup> , T
	6.88-7.02	C
KA3575	1.03-1.27	C, D+P, T
	6.98-7.12	C
KA3581	1.10-1.33	C, (D+P) <sup>*</sup> , T
	6.80-6.95	C
KA3587	0.97-1.14	C, D+P, T
	7.12-7.25	C
KA3593	1.42-1.63	C, (D+P) <sup>*</sup> , T
	4.19-4.43 xenolith	C, D+P, T
	6.93-7.12	C

<sup>\*</sup>) Two determinations on two separate samples.

The results have been evaluated with respect to existing conditions when the measurements were carried out. Comparisons have been made between laboratory and field results as well as results of previous studies.

## **5 Description of Methods**

### **5.1 Laboratory Analysis of Density and Porosity**

Selected rock samples were examined in the laboratory with respect to density and water absorption. Water absorption is a measure of the amount of water that can be gathered in pores. In a sense, the measured water absorption can be approximated with the porosity of the samples (pore volume in relation to total volume).

The density was determined according to standards, DIN 52102-RE VA. The water absorption was determined according to standards, DIN 52103-A. Water absorption was also determined after boiling the samples in water for 5 hours followed by drying of the samples. The reason for this was to remove possible air. It was of interest to study whether this treatment would affect the pores of the rock and produce different water absorption results. Evaluations of water absorption were made with and without consideration of measured weight loss during water storage and boiling.

The investigations were performed by the Swedish National Testing and Research Institute (SP).

### **5.2 Analysis of Chemical and Mineralogical Composition**

The geochemical data were determined using ICP analyses. Samples were also selected for mineralogical analyses using SEM and EDS techniques.

Inductively Coupled Plasma (ICP) is an analytical technique used for the detection of trace metals in environmental samples, such as rocks. The plasma is actually a gas in which atoms are present in an ionized state. ICP in conjunction with mass spectrometry, utilizes a high temperature argon plasma to excite the atoms of the elements present in the introduced solution. By using ICP several elements can be determined simultaneously. Sample preparation includes crushing and grinding of the sample.

In scanning electron microscopy (SEM) an electron beam is scanned across a sample's surface. When the electrons strike the sample, a variety of signals are generated, and it is the detection of specific signals which produces an image of a sample's elemental composition. Interactions of the electron beam with atoms in the sample also result in the emission of X-rays. The emitted X-ray has an energy characteristic of the parent element. Detection and measurement of this energy using energy dispersive spectroscopy permits elemental analysis of the sample. Energy dispersive spectroscopy (EDS) can provide quantitative analysis of elemental composition with a sampling depth of 1-2

microns. The emitted X-rays can also be used to show the elemental distribution in a sample surface.

Investigations and evaluations of geochemical and mineralogical compositions were performed by Terralogica AB.

### 5.3 Laboratory Measurements of Thermal Properties

Measurements of thermal properties in the laboratory were performed using the TPS method (Gustafsson, 1991). The TPS (transient plane source) method is used for measurements of thermal diffusivity and thermal conductivity of both fluids and solids, from cryogenic temperatures to about 250 °C (if the insulation is made of kapton). The thermal conductivity that can be measured ranges from 0.01 W/m°C to 400 W/m°C.

The method uses a sensor element with an engraved pattern of a thin double spiral. The spiral is made of Ni metal and has specific resistivity properties. The spiral is embedded between two layers of kapton, to give it mechanical strength and electrical insulation whereas measurements may be performed in electrically conductive materials. The total thickness of the sensor is 0.025 mm and for this specific application the diameter was 20 mm. The probing depth in a transient experiment should be of the same order as the diameter of the hot disk.

Measurements are performed by placing the sensor between two samples of the same material. The surfaces of the samples have to be smooth in order to limit the contact resistance between the sensor and the sample surfaces. During the measurement, the sensor acts both as a heat generator of a heat pulse and as sensor for the temperature response. The temperature is measured in 200 points across the sensors surface.

The evaluation uses the fact that the resistance for a thin Ni spiral at any time is a function of its initial resistance, the temperature increase and the temperature coefficient of the resistivity. Expressions of the mean temperature increase of the sensor, assuming perfect contact with the sample surfaces, are stored in the software. By fitting measured temperatures with a theoretical temperature development, through a number of iterations, the thermal diffusivity and thermal conductivity are determined.

The accuracy of the thermal conductivity measurements is better than 5 % for the interval 0.01-400 W/m°C, and the repetitiveness is better than 2 % according to the manufacturer.

#### **Test procedure**

Rock samples from core drillings have a diameter of about 45 mm. The selected samples were cut in two halves, each with a thickness of about 15 mm. The two intersection surfaces were then carefully polished.

All samples were measured with respect to thermal diffusivity and thermal conductivity at room temperature 21 °C. A selection of the samples were also measured at 0 °C and at temperatures around 50 °C and 75 °C.

For each sample, at least three measurements were performed at 0 °C and at room temperature (21 °C). Thermal properties are presented as a mean value of these measurements. The sensor was dismantled after each measurement, in order to regain thermal balance before the next measurement. The temperature 0 °C was achieved by placing the sample in an ice bath.

Measurements at elevated temperatures were performed by placing the sample in a water bath with a temperature of 80 °C. Cooling of the sample was taking place at a very slow rate. The temperature was measured to determine the cooling rate. Measurements of thermal properties were performed at different temperatures and thermal properties were evaluated with respect to the continuous cooling of the sample in the water bath. The sensor was never dismantled between the measurements.

Measurements were performed after water saturation of the samples in a water bath. In order to achieve water saturation, the samples were placed in boiled water, first semi-immersed for 24 hours followed by 24 hours completely immersed. The same procedure as for the water absorption measurements was used. The measurements at room temperature were also performed under dry conditions. However, these measurements were performed at a lower accuracy.

Measurements of thermal properties in the laboratory were performed by CIT Thermo-flow AB.

## **5.4 Field Measurements of Thermal Properties**

Measurements of thermal conductivity were performed in accordance with the so called multi-probe method (Sundberg, 1988). This method makes it possible to simultaneously determine the thermal diffusivity of the rock mass since measurements are performed over a certain rock volume. Properties may also be measured simultaneously in different directions with this method. The method is fully described in report "Field measurements of thermal properties of the rocks in the prototype repository at Äspö HRL" (Sundberg & Gabriellsson, 1998).

The method uses the theory of an infinite line source. A heat generating probe is supplied with a constant heat input whereby heat will be dispersed in the ground. The temperature is registered as a function of time by the temperature probes at fixed distances from the heat source. The temperature sensors are situated at half the depth of the heat generating probe in order to reduce boundary effects. The rate of the temperature spread depends on the thermal properties of the surrounding ground. Measured values are used in a numerical solution based on known theories.

The equipment consists of a heat generating probe, a number of small temperature probes, a portable PC, power unit and a logger. Data collection, calculations and graphic presentations of the results are made with special programmes.

### Test procedure

Field work started with the localization of measuring points. The probes were installed in shallow boreholes, 1.2 or 0.6 metres in length corresponding to the length of the heat generating probe and the temperature probes respectively. The boreholes were drilled out with impregnated full cut drills, 16 or 18 mm in diameter, using an electrically driven drilling equipment, see Figure 5-1. In order to secure that boreholes were made parallel, a special drilling frame were used. The frame consisted of two axes perpendicular to each other. It was adjustable in height at the intersection point between the two axes and at the end point of each axis. Measurements were made in two directions, perpendicular to each other. The heat generating probe was installed in origo and the temperature probes at 0.14-0.18 metres distances depending on the conditions at each measuring point.

Photos from the measurements inside the tunnel, showing a typical measurement set-up and a close-up of boreholes with installed probes are shown in Figure 5-2 and Figure 5-3 respectively.

The gap between the probes and the borehole wall was filled with a viscous solution of bentonite, water and quartz sand, in order to reduce the contact resistance. Measurements were performed during 2-3 hours and in some cases overnight. The heat input was set at about 100 W per metre length of probe.

For each measurement installation, variations in the background temperature was registered at a few metres distance by a reference temperature probe at the measurement level, 0.6 metres depth.

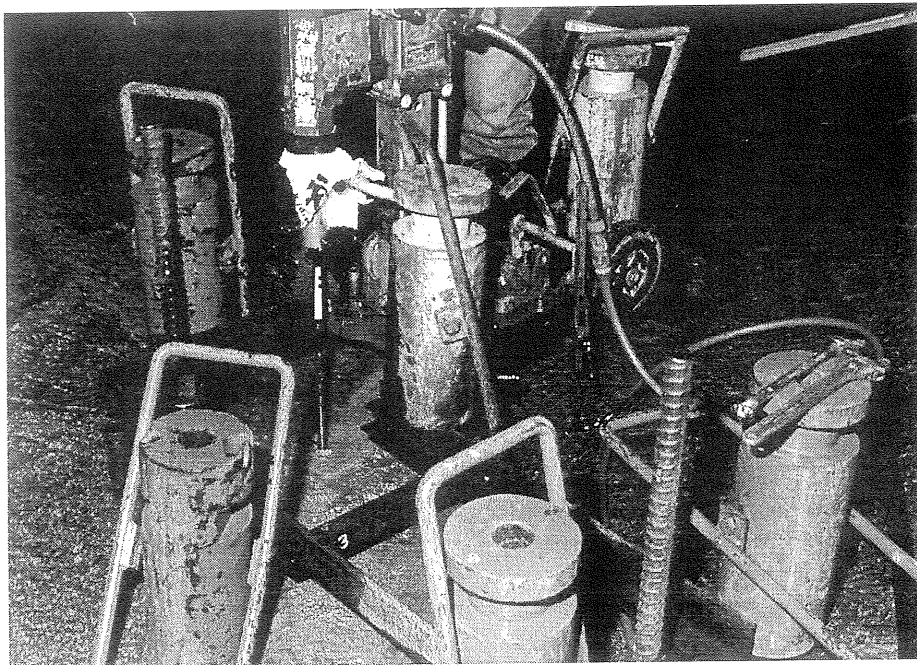


*Figure 5-1 Drilling of boreholes for thermal probe measurements in the tunnel for the Prototype Repository at Äspö.*

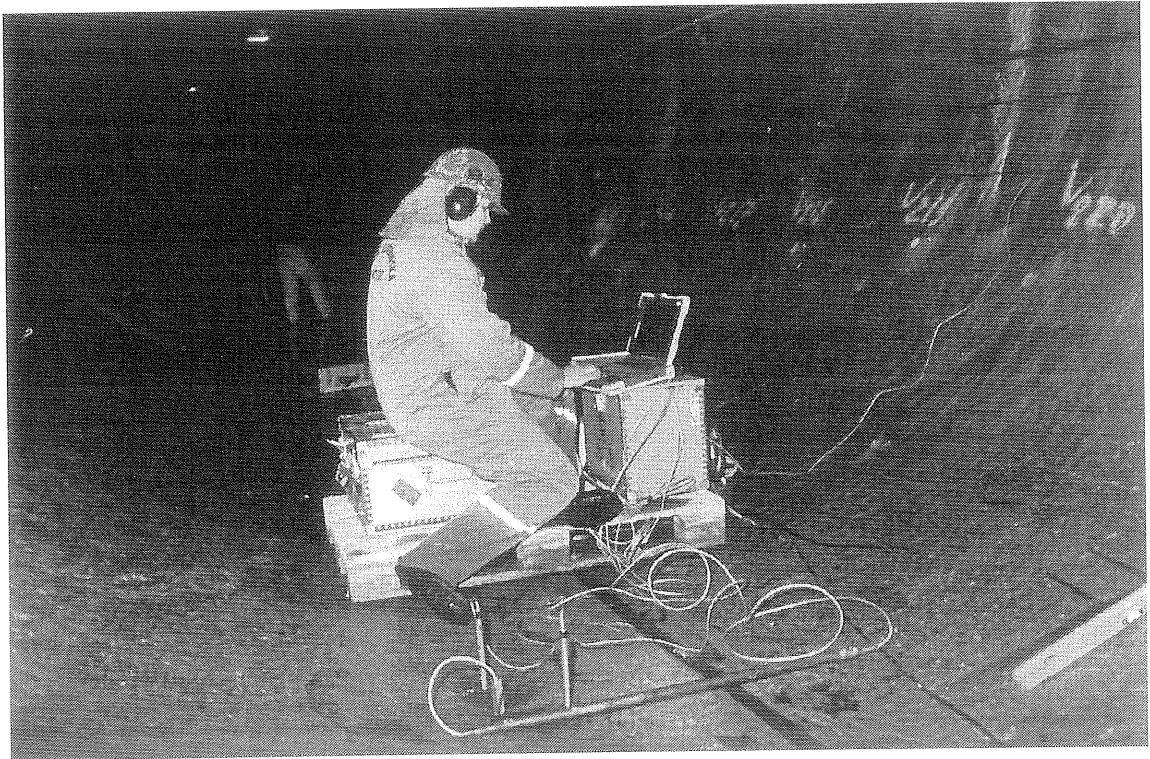


*Figure 5-2 Thermal probe measurements of thermal properties of the rocks in the tunnel for the Prototype Repository at Äspö.*

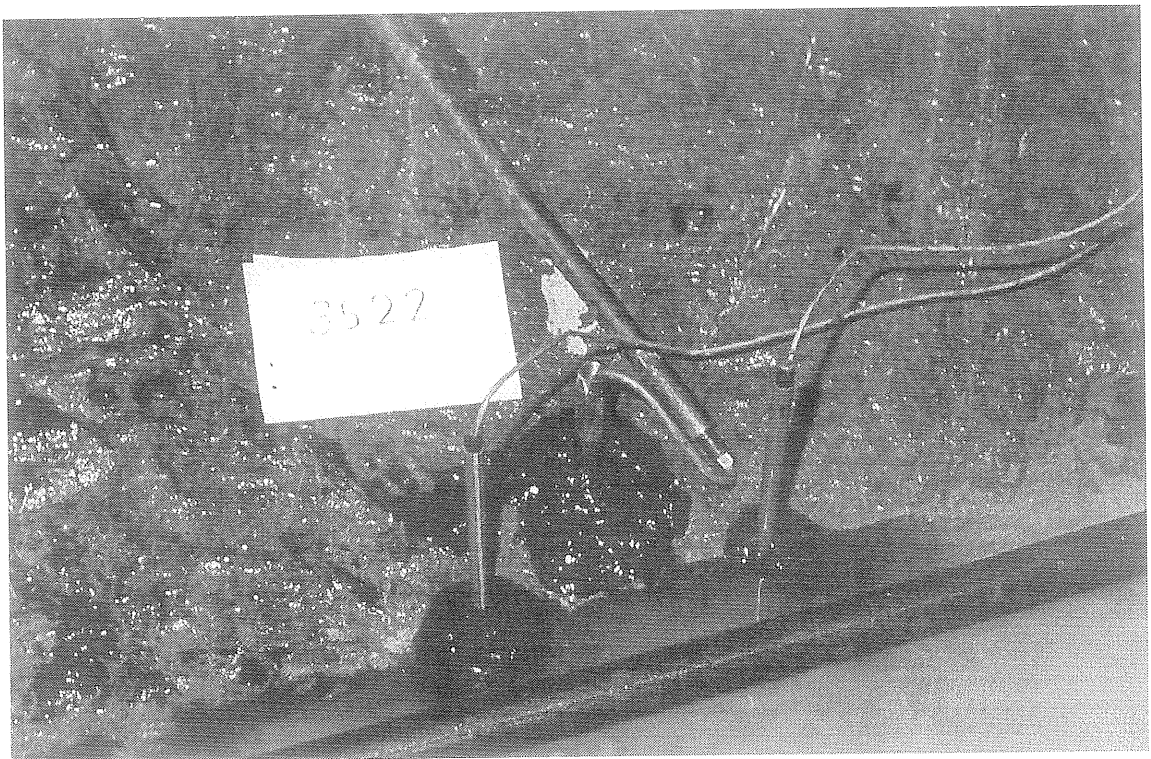


*Figure 5-3 Boreholes with installed probes at section 3522. Installations in a dyke of mylonite. The heat generating probe is situated in the centre and two temperature probes at about 0.16 metres from the centre probe.*

## 5.5 Computer Calculations of Thermal Conductivity

The thermal conductivity was calculated with the Condrock programme (Sundberg, 1991:2). Condrock calculates the thermal conductivity of isotropic rock at normal temperature, about 10 °C. The thermal conductivity of the rock is calculated using reference values of the thermal conductivity of different minerals together with the volume fractions as input. The numerical solution is based on the self-consistent approximation which has previously proved to be in good agreement with measured values (Sundberg, 1988).

The thermal conductivity of plagioclase, as well as olivine and pyroxene, depends on the chemical composition and may therefore vary within certain intervals.



## 6 Density and Porosity

The average density considering all Äspö diorite samples is  $2750 \text{ kg/m}^3$ . The density of the 10 Äspö diorite samples (14 determinations) varies between  $2713\text{-}2815 \text{ kg/m}^3$ .

The density of the xenolith sample was measured at  $2820 \text{ kg/m}^3$ .

Density and water absorption of rock samples are shown in Figure 6-1. Water absorption is assumed to be equal to the porosity of the samples.

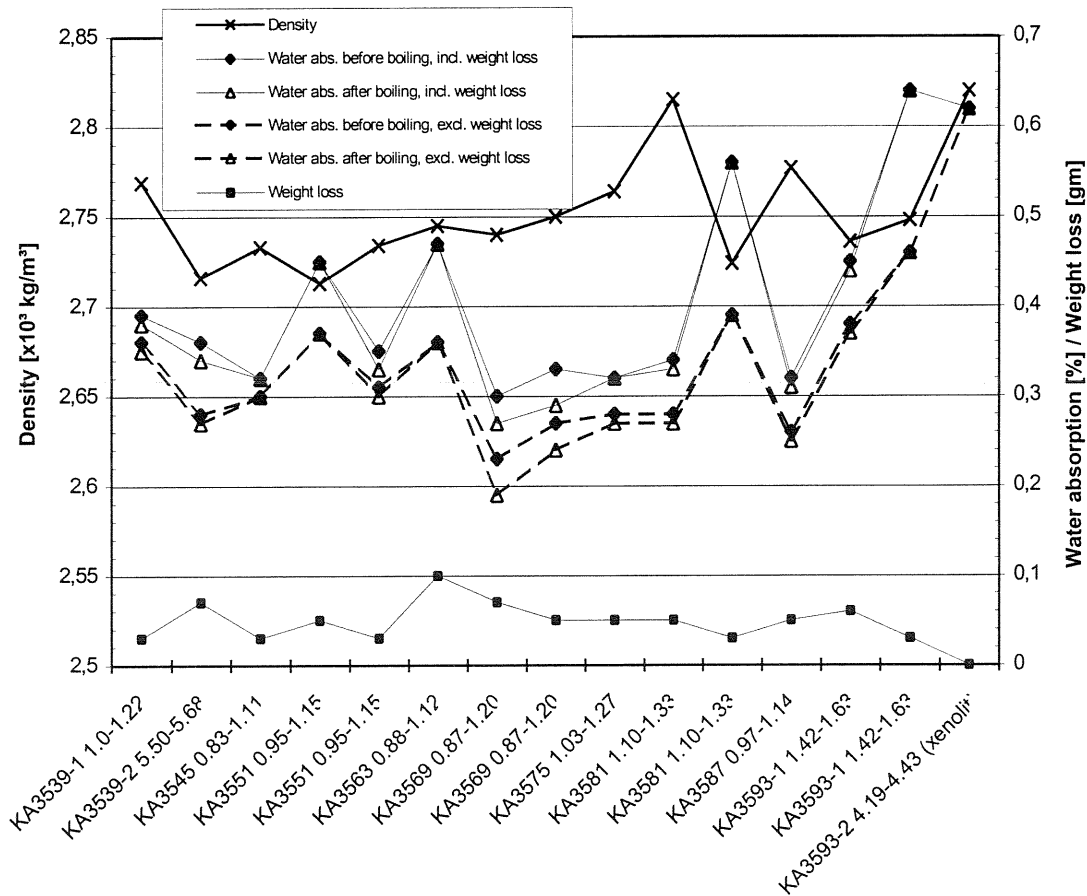


Figure 6-1 Density and water absorption of Äspö diorite and xenolith. Results from laboratory examinations of rock samples.

Two determinations were made using samples KA3551 0.95-1.15, KA3569 0.87-1.20, KA3581 1.10-1.33 and KA3593-1 1.42-1.63. Separate samples were used for each determination. In Figure 6.1 it is noticed that especially the water absorption results vary for samples with the same name. For KA3581 1.10-1.33, the water absorption was measured at 0.34 in one sample and at 0.56 in the other sample (before boiling, includ-



ing weight loss). This variation corresponds to a lower density for the sample with higher water absorption properties.

Mean values of the water absorption, including standard deviations and spreading intervals for the Äspö diorite samples are compiled in Table 6-1. Water absorption for the xenolith sample was measured at 0.62 % before and after boiling.

**Table 6-1 Mean values and spreading intervals of the water absorption (volumetric %) before and after boiling the Äspö diorite samples in water for 5 hours, and with and without consideration of weight loss during water storage and boiling.**

	Mean value	Standard deviation	Interval
Water absorption before boiling, no consideration of weight loss	0.32	0.064	0.23-0.46
Water absorption after boiling, no consideration of weight loss	0.31	0.072	0.19-0.46
Water absorption before boiling with consideration of weight loss	0.40	0.102	0.30-0.64
Water absorption after boiling with consideration of weight loss	0.39	0.109	0.27-0.64

Weight loss for the Äspö diorite samples after water storage and boiling varied between 0.03-0.10 grams, in average 0.2 % of the total sample weight. Weight loss for the xenolith sample was not measured.

Some of the samples represent Äspö diorite that has certain degree of alteration and other samples represent relatively fresh Äspö diorite. The subdivision of samples is discussed in Chapter 7. The average density for the altered Äspö diorite samples (KA3539-2 5.50-5.68, KA3545 0.83-1.11 and KA3551 0.95-1.15) is somewhat lower (1-2 %) than for the fresh Äspö diorite samples (KA3563 0.88-1.12, KA3581 1.10-1.33 and KA3587 0.97-1.14), see Table 6-2.

**Table 6-2 Mean values and standard deviation of the density (kg/m<sup>3</sup>) for altered and fresh Äspö diorite and xenolith.**

Rock	Mean value	Standard deviation	Interval
Fresh Äspö diorite <sup>1</sup>	2765	39.7	2724 - 2815
Altered Äspö diorite <sup>2</sup>	2724	11.0	2713 - 2734
Xenolith	2820	-	-

1) Sample KA3563 0.88-1.12, KA3581 1.10-1.33 (two samples) and KA3587 0.97-1.14.

2) Sample KA3539-2 5.50-5.68, KA3545 0.83-1.11 and KA3551 0.95-1.15 (two samples).

Water absorption of altered and fresh Äspö diorite is shown in Table 6-3. Determinations before and after boiling produced about the same results. However, a certain difference is noticed dependent on whether weight loss, during water storage and boiling,

is considered or not. Higher water absorption values is obtained when weight loss is considered.

In Table 6-3 a small difference in water absorption between fresh and altered Äspö diorite is noticed when weight loss is considered. The water absorption of one of the fresh Äspö diorite samples (KA3581 1.10-1.33) was significantly higher than for the other samples. If this sample is not included in the mean value, the water absorption of the fresh Äspö diorite becomes in the same order as for the altered Äspö diorite.

**Table 6-3 Mean values of the water absorption (volumetric %) for altered and fresh Äspö diorite and xenolith. Before and after boiling, with and without consideration of weight loss during water storage and boiling. Standard deviations are written between brackets.**

Rock	Before boiling		After boiling	
	excl weight loss	incl weight loss	excl weight loss	incl weight loss
Fresh Äspö diorite <sup>1</sup>	0.32 (0.062)	0.42 (0.113)	0.32 (0.068)	0.42 (0.119)
Altered Äspö diorite <sup>2</sup>	0.32 (0.039)	0.37 (0.056)	0.31 (0.042)	0.36 (0.061)
Xenolith	0.62	0.62	0.62	0.62

3) Sample KA3563 0.88-1.12, KA3581 1.10-1.33 (two samples) and KA3587 0.97-1.14.

4) Sample KA3539-2 5.50-5.68, KA3545 0.83-1.11 and KA3551 0.95-1.15 (two samples).

A compilation of density and water absorption results is given in Appendix 3.

## 7 Mineral Composition

All samples (19 in total) representing Äspö diorite show various degrees of alteration, In some samples biotite is completely replaced by chlorite, and plagioclase by albite, epidote and sericite (saussuritisation).

In order to determine the two extremes, two samples representing relatively fresh Äspö diorite (KA3563 0.88-1.12 and KA3587 0.97-1.14) and three samples representing altered Äspö diorite (KA3539 5.50-5.68, KA3545 0.83-1.11 and KA3551 0.95-1.15) were selected. Average values of chemical composition from the two groups are given in Table 7-1. Chemical data for each sample is presented in Appendix 4.

**Table 7-1 Geochemical data of rock samples representing fresh Äspö diorite (ÄD) and altered Äspö diorite respectively.**

	Fresh ÄD <sup>1</sup>	Altered ÄD <sup>2</sup>
SiO <sub>2</sub> %	59.9	58.5
Al <sub>2</sub> O <sub>3</sub>	17.7	17.5
CaO	4.82	3.96
Na <sub>2</sub> O	4.53	3.88
Fe <sub>2</sub> O <sub>3</sub>	5.79	6.24
K <sub>2</sub> O	3.21	3.99
MgO	2.44	2.89
MnO <sub>2</sub>	0.10	0.126
P <sub>2</sub> O <sub>5</sub>	0.35	0.359
TiO <sub>2</sub>	0.86	0.917
LOI	1.25	2.1
Ba ppm	1625	1513
Nb	31.7	36.3
Sr	1340	1247
Y	23.6	27.1
Zr	248	263

1) *Samples KA3563 0.88-1.12 and KA3587 0.97-1.14.*

2) *Samples KA3539 5.50-5.68, KA3545 0.83-1.11 and KA3551 0.95-1.15.*

Loss of Ca, Na and Sr in the altered samples is explained by breakdown of plagioclase. LOI (loss of ignition) corresponds to crystal bound water or carbonates and sulphides. The LOI values are significantly higher in the altered samples because of the higher

chlorite content. The redstaining of the altered samples are due to micrograins of hematite/Fe-oxyhydroxide hosted in the feldspars. Mostly, Äspö diorite with high degrees of alteration is more redstained than fresh Äspö diorite.

The chemical analyses of the 19 Äspö diorite samples are largely similar. In contrast, the microscopy reveals significant variations in mineralogical composition due to various degrees of alteration in the different samples. One fresh Äspö diorite sample (KA3581 1.10-1.33) was treated separately because of significant differences compared with the other samples. Mineralogical composition based on microscopy are shown in Table 7-2.

**Table 7-2 Mineralogical composition of rock samples representing fresh Äspö diorite (ÄD), altered Äspö diorite and xenolith, based on microscopy and chemical composition.**

	Fresh ÄD <sup>1</sup>	Fresh ÄD <sup>2</sup>	Altered ÄD <sup>3</sup>	Metabasite xenolith <sup>4</sup> sample
Quartz	10	10	11	6
K-feldspar	10	10	16	6
Plagioclase	52 (c. 25%An)	50	34 (albite)	35 (c. 30% An)
Biotite	18	15	-	25
Chlorite	-	-	20	1
Sericite	1	1	6	1
Epidote	7	7	12	19
Hornblende	1	5	-	6
Titanite	1	1	1	1
Apatite	+	+	++	+
Calcite	+	+	+	-
Magnetite	+	+	+	+

+ Minerals observed, but constituting less than 1 %.

1) Samples KA3563 0.88-1.12 and KA3587 0.97-1.14.

2) Sample KA3581 1.10 - 1.33.

3) Samples KA3539 5.50-5.68, KA3545 0.83-1.11 and KA3551 0.95-1.15.

4) Sample KA3593-2 4.19-4.43.

SEM/EDS analyses of fresh plagioclases in samples KA3581 and KA3587 showed between 25-27 % of anorthite (An). Based on calculation, the An content in the metabasite hybride, xenolith, may be just slightly higher (c. 30 % An).

All the Äspö diorite samples, except for KA3539 5.50-5.68, KA3545 0.83-1.11 and KA3551 0.95-1.15 (the altered samples referred to above), have biotite as the dominating femic mineral. Minor amounts of hornblende are present in some of the samples as well as pumpellyite. For example, sample KA3581 1.10-1.33 is a fresh Äspö diorite

sample with relatively high content of hornblende reflected in the relatively high  $\text{Fe}_2\text{O}_3$  content (6.17 weight %) corresponding to a low LOI content (0.9 weight %), see Table 7-1. Sample KA3593 1.42-1.63 has biotite which in parts of the sample contains pumpepyrite.

The plagioclase shows various degrees of saussuritisation, also within the samples having biotite preserved. Sample KA3539 1.0-1.22, KA3569 0.87-1.20 and KA3575 1.03-1.27 all have mineralogical composition similar to that of fresh Äspö diorite except for a slight albitisation and in addition they may have somewhat higher epidote contents.

## 8 Thermal Properties

### 8.1 Results from Laboratory Measurements

Thermal properties measured in the laboratory at room temperature, 21 °C, are shown in Figure 8-1. Measurements at dry conditions were made with less accuracy than at saturated conditions. Results from all laboratory measurements of thermal properties are compiled in Appendix 5.

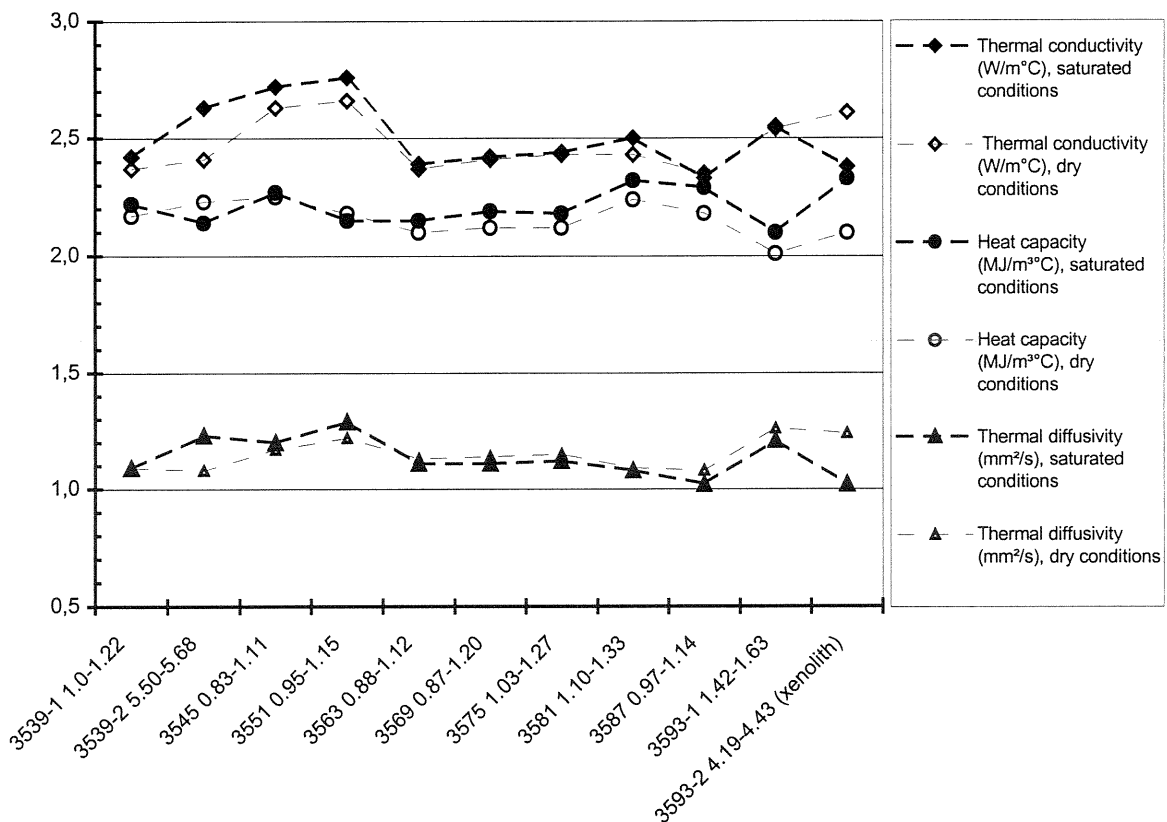


Figure 8-1 Thermal properties of rock samples. Results from measurements at a temperature of 21 °C, with dry and saturated samples.

Thermal properties, presented as mean values and spreading intervals for the Äspö diorite samples, at saturated and dry conditions are summarized in Table 8-1.

**Table 8-1 Mean values of thermal properties and spreading intervals based on 10 rock samples of Äspö diorite. Results at a temperature of 21 °C, dry and saturated conditions.**

	Thermal conductivity [W/m°C]		Thermal diffusivity [mm <sup>2</sup> /s]		Heat capacity [MJ/m <sup>3</sup> °C]	
	saturated	dry	saturated	dry	saturated	dry
Mean value	2.52	2.46	1.15	1.14	2.20	2.16
Spreading interval	2.33-2.76	2.35-2.66	1.02-1.29	1.08-1.29	2.10-2.32	2.01-2.25

The thermal conductivity for the xenolith sample was measured at 2.38 W/m°C at saturated conditions, and at 2.61 at dry conditions. Corresponding values of thermal diffusivity were measured at 1.02 mm<sup>2</sup>/s and at 1.24 mm<sup>2</sup>/s. Results from the measurements resulted in calculated heat capacities of 2.33 MJ/m<sup>3</sup>°C at water saturation, and of 2.1 MJ/m<sup>3</sup>°C at dry conditions.

Results from laboratory measurements of thermal properties at various temperatures are shown in Figure 8-2, Figure 8-3 and Figure 8-4.

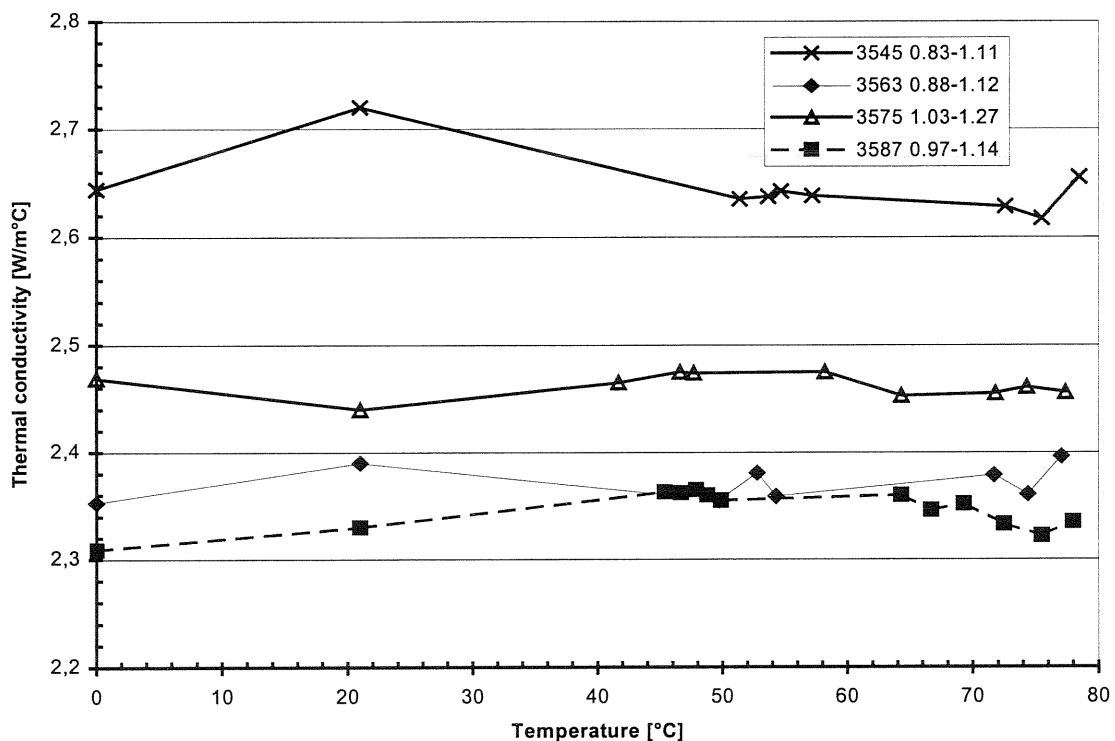


*Figure 8-2 Thermal conductivity of Äspö diorite at different temperatures. From measurements in the laboratory.*

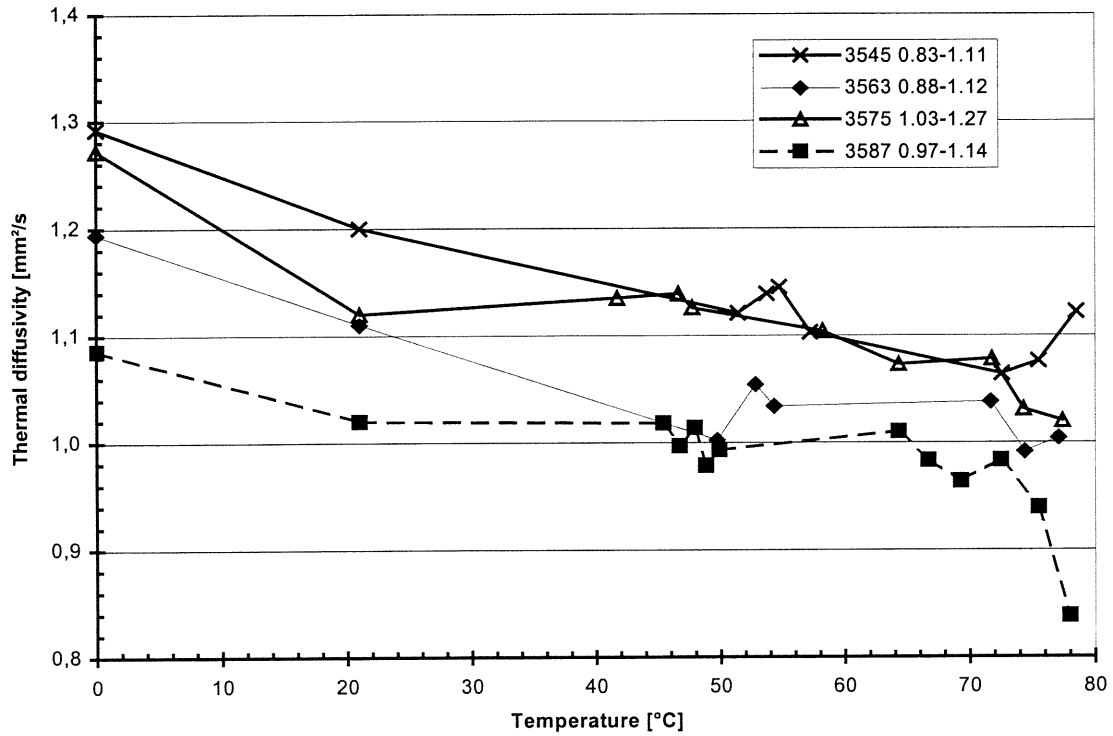


Figure 8-3 Thermal diffusivity of Äspö diorite at different temperatures. From measurements in the laboratory.

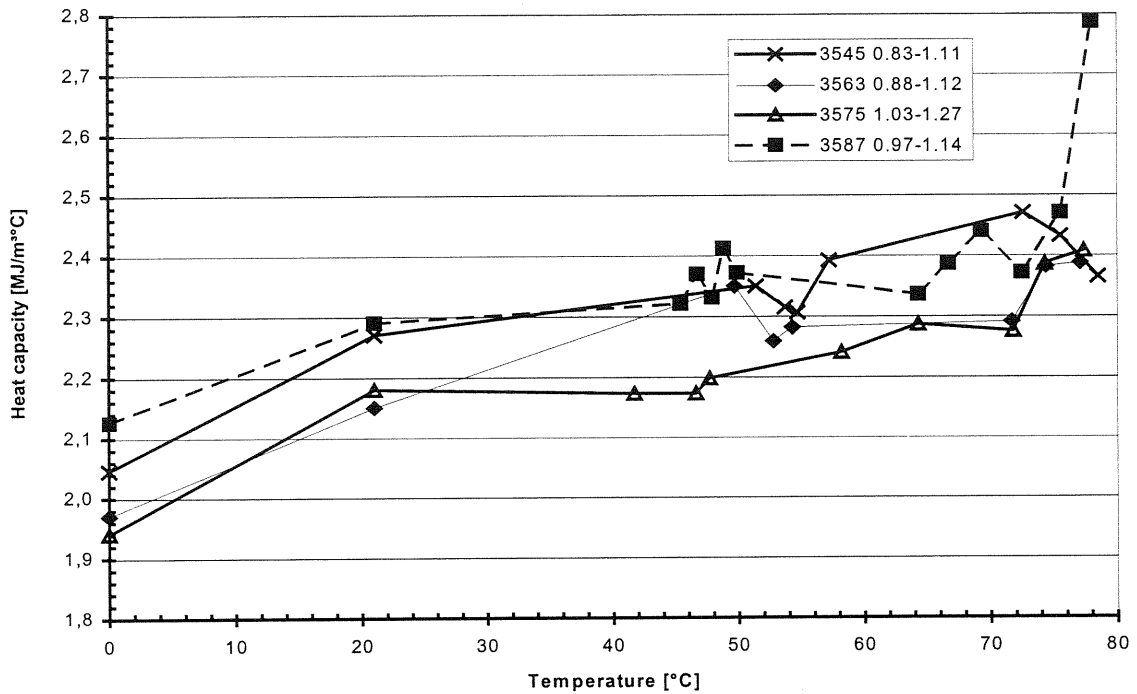


Figure 8-4 Heat capacity of Äspö diorite obtained from measurements of thermal conductivity and thermal diffusivity in the laboratory.



### **Practical experiences**

When performing the measurements one should take careful notice of the position of the sensor, especially if several measurements are performed with the same pair of samples. The sensor should be positioned in the same place.

## **8.2 Results from Field Measurements**

Field measurements of thermal properties were performed in January 1998, at six different locations in the Prototype Repository tunnel, at section 3522, 3525, 3535, 3566, 3583 and 3594. The reference temperature was measured in boreholes at section 3529 and 3574. The boreholes were drilled out outgoing from the tunnel floor. Co-ordinates for each measurement hole are listed in "Appendix 6: Co-ordinates of boreholes and layout at the thermal probe measurement points".

The results from the field measurements have previous been compiled and evaluated in report "Field measurements of thermal properties of the rocks in the prototype repository at Äspö HRL" (Sundberg & Gabrielsson, 1998).

Measurements were performed in Äspö diorite at four out of six locations, at one location in a dyke of mylonite and at one location with a local intrusion of fine-grained granite. One measurement was made over a wide structure, in section 3594 (No. 2), and over a smaller joint, possibly filled with epidote, at section 3566 (No. 2).

The results of the thermal probe measurements are shown in Table 8-2.

Some of the measurements were disturbed by water flow in the boreholes and adjacent fissures. The water flow probably cooled down the probes whereby the measured rate of temperature increase was lowered compared with conditions without water flow. This resulted, for example, in unreasonably high values of the thermal conductivity of the rock.

Measurements in certain rocks with a limited extension may partly have taken place in adjacent rocks (e.g. in section 3525).

The field measurements in Äspö diorite produced values in the same order, except at section 3566 (No. 1) where higher values were obtained. Nearby, there is a fracture filled with epidote which indicates that the rock in this section is not as homogenous as for the other sections with Äspö diorite.

Data and graphical plots for each measurement set-up are presented in "Appendix 7: Data and graphic presentations of results from thermal probe measurements".

The difference between start and end values of the background temperature amounted to about 0.01 °C during evaluation periods. These variations do not influence the evaluations of the thermal properties.

**Table 8-2 Thermal properties of the rocks measured with thermal probes. Values in brackets were obtained at conditions with high water flows.**

Section	Thermal Conductivity [W/m°C]		Thermal Diffusivity [mm <sup>2</sup> /s]		Calculated Heat capacity [MJ/m <sup>3</sup> °C]		Type of rock and additional remarks
	No. 1	No. 2	No. 1	No. 2	No. 1	No. 2	
3522	3.16		1.44		2.19		Mylonite
		3.16		1.39		2.27	Mylonite
3525	2.72		1.22		2.23		Small area of fine-grained granite.
		2.71		1.21		2.24	Small area of fine-grained granite.
3535 (Meas. No. 1)	2.73		1.27		2.15		Äspö diorite
		(3.49)		(1.28)		(2.73)	Äspö diorite. Meas. disturbed by water flow.
3535 (Meas. No. 2)	2.67		1.17		2.28		Äspö diorite
		(3.76)		(1.39)		(2.71)	Äspö diorite. Meas. disturbed by water flow.
3566	3.16		1.51		2.09		Äspö diorite
		3.19		1.45		2.20	Äspö diorite crossed by possibly epidote.
3583	2.80		1.16		2.41		Äspö diorite
		2.78		1.29		2.16	Äspö diorite
3594	(5.98)		(1.45)		(4.12)		Äspö diorite. Meas. disturbed by water flow.
		(3.64)		(1.23)		(2.96)	Äspö diorite, over structure. Meas. probably disturbed by water.

### Practical experiences

The drilling equipment together with the special drilling frame produced fairly parallel boreholes. Drilling of boreholes is time-consuming. Time spent for the drilling of two boreholes down to 0.6 metres and one borehole down to 1.2 metres depth was 3-4 hours. The homogenous rock mass together with small diameter boreholes result in high restrictions on the drilling equipment. The electric drilling unit broke down at one occasion.

It may be concluded that measurements over structures and fractures are more difficult to perform. Drilling may cause cracks and open up for the release of water pressure/flow. This effect is more evident at large depths in the rock and where water pressure gradients are high.

### 8.3 Thermal Properties from Calculations

Results from calculations of the thermal conductivity of fresh and altered Äspö diorite, and xenolith, are presented in Table 8-3.

**Table 8-3 Calculated thermal conductivity of fresh Äspö diorite, altered Äspö diorite and xenolith. Results from Condrock calculations.**

Rock type	Thermal conductivity [W/m°C]
Fresh Äspö diorite <sup>1</sup>	2.21
Fresh Äspö diorite <sup>2</sup>	2.24
Altered Äspö diorite <sup>3</sup>	3.20
Xenolith <sup>4</sup>	2.27

1) Samples KA3563 0.88-1.12 and KA3587 0.97-1.14.

2) Sample KA3581 1.10 - 1.33.

3) Samples KA3539 5.50-5.68, KA3545 0.83-1.11 and KA3551 0.95-1.15.

4) Sample KA3593-2 4.19-4.43.

The calculations are based on mineralogical compositions (Chapter 7) and reference values of the thermal conductivity of different minerals, see Table 8-4.

**Table 8-4 Minerals found in samples of Äspö diorite (ÄD) and corresponding thermal conductivity used for the calculations (Horai and Simmons, 1969, and Horai, 1971). Values in brackets are estimations.**

	Fresh ÄD <sup>1</sup>		Fresh ÄD <sup>2</sup>		Altered ÄD <sup>3</sup>		Xenolith <sup>4</sup>	
	[%]	[W/m°C]	[%]	[W/m°C]	[%]	[W/m°C]	[%]	[W/m°C]
Quartz	10	7.69	10	7.69	11	7.69	6	7.69
K-feldspar	10	2.51	10	2.51	16	2.51	6	2.51
Plagioclase	52	1.61 (c. 25% An)	51	1.61 (c. 25% An)	34 (albite)	2.1	35 (c. 30% An)	1.56
Biotite	18	2.0	15	2.0	-	-	25	2.0
Chlorite	-	-	-	-	20	5.1	1	5.1
Sericite*	1	2.3	1	2.3	6	2.3	1	2.3
Epidote	7	2.8	7	2.8	12	2.8	19	2.8
Hornblende	1	2.8	5	2.8	-	-	6	2.8
Titanite	1	3.0	1	3.0	1	3.0	1	3.0

\*) The thermal conductivity of sericite is unknown. Sericite resembles muscovite and the thermal conductivity is therefore estimated to be the same as for muscovite.

1) Samples KA3563 0.88-1.12 and KA3587 0.97-1.14.

2) Sample KA3581 1.10 - 1.33.

3) Samples KA3539 5.50-5.68, KA3545 0.83-1.11 and KA3551 0.95-1.15.

4) Sample KA3593-2 4.19-4.43.

Variations of  $\pm 2$  % in An-content of fresh Äspö diorite result in variations of the thermal conductivity less than 1 %.

The chlorite content in the altered Äspö diorite has a significant influence on the total thermal conductivity. For a  $\pm 5$  % variation of the chlorite content, the calculated thermal conductivity varies by  $\pm 3$  %. Examinations of the altered Äspö diorite sample 3545 0.83-1.11 show that this sample has somewhat lower chlorite content. By assuming a chlorite content of 15 % (hornblende 4 % and magnetite 1 %) the thermal conductivity is calculated at 3.12 W/m°C.

## 9 Evaluation and Discussion

### 9.1 Comparisons between Laboratory, Field and Calculated Results

A number of measurements of thermal properties have been performed in Äspö diorite, which is the dominating rock around the Prototype Repository tunnel at Äspö. Thermal properties measured in the field differ from those measured in rock samples in the laboratory and also from the calculated values. There are also significant variations within each measurement method.

The thermal conductivity of the Äspö diorite measured in the laboratory and in the field, as well as results from calculations are shown in Figure 9-1. The values measured in the field are generally higher than those measured in the laboratory, the mean difference being about 12 %. Calculated values are both higher and lower than the measured values.

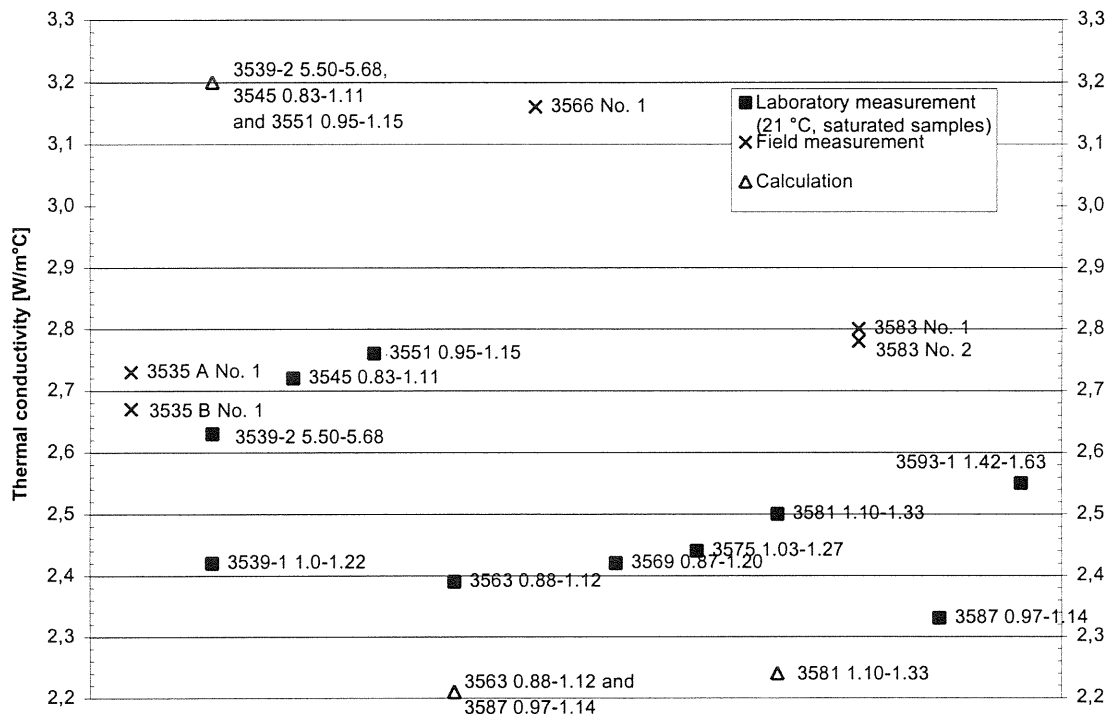


Figure 9-1 Thermal conductivity of Äspö diorite from laboratory (21 °C, saturated conditions) and field measurements, and calculations based on mineral composition. Samples 3539-2 5.50-5.68, 3545 0.83-1.11 and 3551 0.95-1.15 represent altered Äspö diorite. Samples 3563 0.88-1.12, 3581 1.10-1.33 and 3587 0.97-1.14 represent fresh Äspö diorite.

The samples showed different degrees of alteration, from relatively fresh Äspö diorite to altered Äspö diorite. Calculations of thermal conductivity were made for two extremes. The calculated values of Figure 9-1 are thus based on average mineral compositions of several samples. Samples 3539-2 5.50-5.68, 3545 0.83-1.11 and 3551 0.95-1.15 represent altered Äspö diorite. Samples 3563 0.88-1.12, 3581 1.10-1.33 and 3587 0.97-1.14 represent fresh Äspö diorite. The calculated thermal conductivity of altered Äspö diorite is significantly higher than the results from the measurements (see Figure 9-1). The calculated thermal conductivity of fresh Äspö diorite is on the contrary lower than the measured values.

Measured thermal conductivity of samples with an apparent alteration is higher than the thermal conductivity of fresh Äspö diorite. The calculations also resulted in higher thermal conductivity values for the altered Äspö diorite compared with the fresh Äspö diorite, due to a higher content of chlorite.

The majority of the field measurements is best in agreement with the laboratory results for the altered Äspö diorite. However, the degree of alteration for the Äspö diorite at the different measurement points is not known.

The majority of the thermal diffusivity values is between 1-1.3 mm<sup>2</sup>/s, see Figure 9-2. The measured field values are mainly in the upper part of the interval and the laboratory values are in the lower part of the interval. The thermal diffusivity is generally higher for the altered Äspö diorite than for the fresh Äspö diorite, based on laboratory measurements.

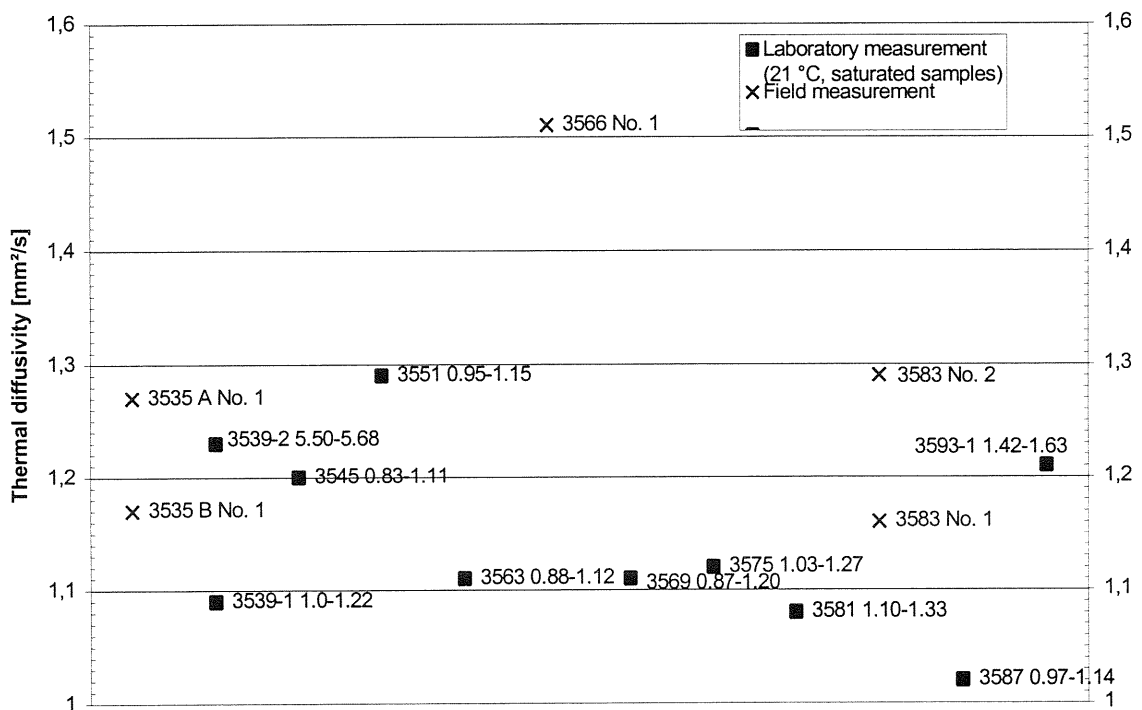


Figure 9-2 Thermal diffusivity of Äspö diorite from laboratory (21 °C, saturated conditions) and field measurements.

The heat capacity was calculated using measured values of thermal conductivity and thermal diffusivity, in the field and in the laboratory. The calculated heat capacity of Äspö diorite varies between 2.09-2.42 MJ/m<sup>3</sup>°C, Figure 9-3. There are no clear trends with respect to different types of measurement methods. Values based on field measurements are scattered among the values based on laboratory measurements. The heat capacity is generally somewhat lower for the altered Äspö diorite than for the fresh Äspö diorite.

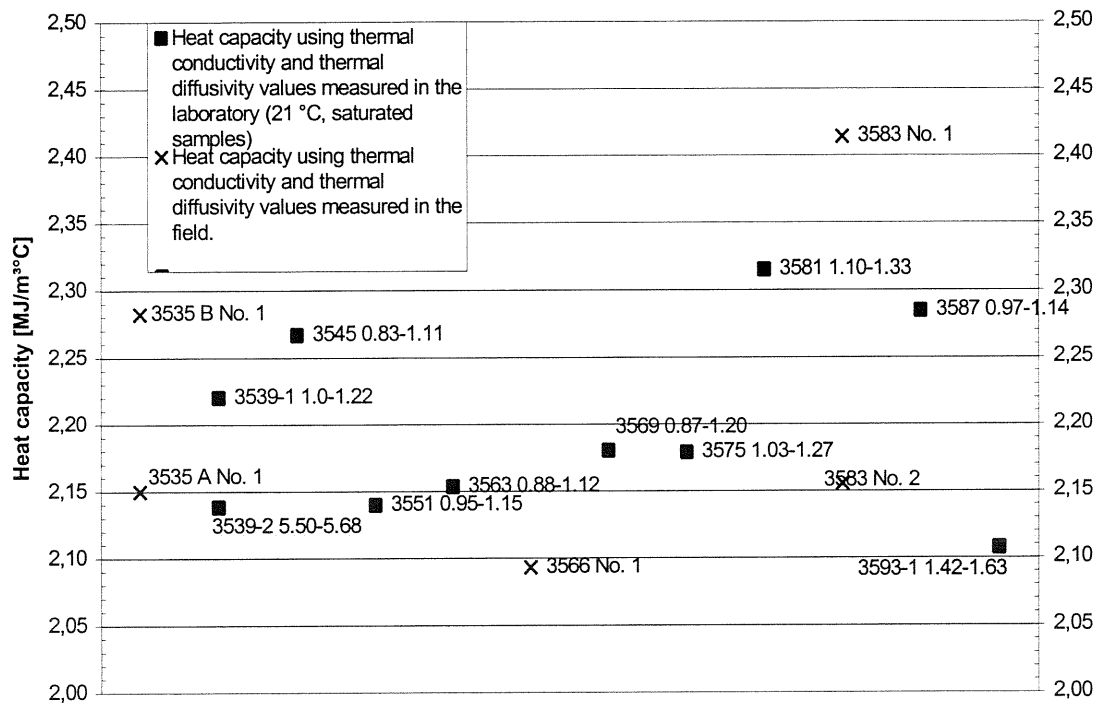


Figure 9-3 Heat capacity of Äspö diorite based on measured values of thermal conductivity and thermal diffusivity in the laboratory (21 °C, saturated conditions) and in the field.

Thermal properties expressed as mean values, considering all results from this study, are shown in Table 9-1.

**Table 9-1 Thermal properties of Äspö diorite (ÄD). Mean values from measurements in the laboratory and in the field. Calculated thermal conductivity based on average mineral compositions.**

	Thermal cond. [W/m°C]		Thermal diffusivity [mm <sup>2</sup> /s]		Heat capacity [MJ/m <sup>3</sup> °C]		Heat capacity [J/kg°C]	
	fresh ÄD	alt. ÄD	fresh ÄD	alt. ÄD	fresh ÄD	alt. ÄD	fresh ÄD	alt. ÄD
Laboratory	2.41	2.70	1.10	1.16	2.25	2.19	814	804
Field <sup>1</sup>	2.83		1.28		2.23 <sup>2</sup>		811 <sup>2</sup>	
Calculation	2.24	3.20	-	-	-	-		

1) Values clearly influenced by observed water flow in boreholes at the measurement points are excluded in the mean value.

2) One heat capacity value differ from the rest (section 3583) and increases the average heat capacity by 3 %.

Laboratory measurements and calculations for the xenolith sample (KA3593-2 4.19-4.43) produced various results. In the laboratory, lower thermal conductivity was measured at saturated conditions (2.38 W/m°C) than at dry conditions (2.61 W/m°C). Normally higher values are expected at saturation because of a higher thermal conductivity of water-filled pores compared with air-filled pores. The measurements at dry conditions were performed at a lower accuracy so it is more likely that this value is incorrect. To investigate this further, additional measurements have to be carried out.

Thermal properties evaluated from field measurements at different sections are summarized in Table 9-2.

**Table 9-2 Thermal properties measured in the field in three different sections in the tunnel for the Prototype Repository.**

Section	Rock type	Thermal conductivity [W/m°C]	Thermal diffusivity [mm <sup>2</sup> /s]	Heat capacity [MJ/m <sup>3</sup> °C]
3522	Mylonite	3.16	1.21	2.61
3525	Fine-grained granite	2.72	1.42	1.92
3566 (No. 2)	Structure of epidote	3.19	1.45	2.20

## 9.2 Temperature Dependence of Thermal Properties

Laboratory measurements of thermal conductivity show no obvious trends with respect to temperature. For one altered sample (KA3545 0.83-1.11) there is a possible trend towards decreasing thermal conductivity values with the temperature (Figure 8-2). Measurements of this sample also resulted in a significantly higher value at room temperature (21 °C) than for the other temperature levels. This value is based on three, or



more, measurements with relatively low spreading. For this reason it is not possible to exclude this value in the evaluation.

Studies of the temperature dependence of the thermal conductivity of common rocks presented in literature have shown a decrease in thermal conductivity with the temperature. The decrease may be in the order of 5-15 % per 100 °C (Sibbit et al, 1979). However, no such temperature dependence is indicated by the results of this study (based on laboratory measurements).

The measured thermal diffusivity in the laboratory decreased with the temperature, in average 15 % within the temperature interval 0-75 °C (Figure 8-3). The thermal diffusivity for sample KA3587 0.97-1.14 at 78 °C differs significantly from the overall decreasing trend. It is much lower.

Consequently, a certain reduction in the thermal diffusivity values with the temperature results in increasing heat capacity values. The heat capacity increases in average by 17 % within the temperature interval 0-75 °C (Figure 8-4). The extremely low value of the thermal diffusivity for sample KA3587 0.97-1.14 at 78 °C consequently results in a very high calculated value of the heat capacity.

An increase of the heat capacity with the temperature has also been reported in the literature. For example in a study by Berman and Brown (1985) the heat capacity of common minerals increased by about 5 % between 25 and 50 °C and by about 10 % between 100 and 200 °C (quartz : 15 %).

### 9.3 Comparisons with Previous Studies

Thermal properties of different rock types at Äspö have previous been calculated based on modal analyses of samples from the rock surface and from boreholes (Sundberg, 1991:1). For the calculations, estimated values of the thermal conductivity of plagioclase and pyroxene were used based on estimations of the chemical composition of these minerals. The heat capacities were calculated as an arithmetic mean value of heat capacities and volume fractions of the constituent minerals. However, heat capacity data was not available for some constituents so estimated values were used. The results are presented in Table 9-3.

The Äspö diorite corresponds closest to group No. 3. A comparison with calculated values in this study shows that the thermal conductivity of fresh Äspö diorite is in average 15 % lower and for altered Äspö diorite it is 20 % higher. The difference in the results compared with Table 9-3 depends, most likely, on different assumptions with respect to mineral compositions. For example in this study it is showed that a chlorite content in the Äspö diorite significantly affects the thermal conductivity.

**Table 9-3 Mean values of thermal conductivity and heat capacity at 25 °C, from calculations based on estimations of mineral composition of different rock types at Äspö (Sundberg, 1991:1).**

Rock type	Thermal conductivity [W/m°C]	Heat capacity [J/kg°C]
1. Greenstone	2.58	775
2. Dioritoids	2.55	770
3. Quartz monzodiorite-granodiorite	2.63	760
4. Granodiorite-granite	3.03	755
5. Granite	3.48	740
All samples	2.96	755

Furthermore, the thermal conductivity in Table 9-3 was calculated for a thermal conductivity of 1.8 W/m°C for the plagioclase which corresponds to an anorthite content of 15 %. In this study, the anorthite content in plagioclase is estimated at 25 % for the fresh Äspö diorite and the corresponding thermal conductivity becomes 1.61 W/m°C. If the value 1.8 W/m°C is used instead, the thermal conductivity of fresh Äspö diorite becomes about 10 % lower (instead of 15 % lower) compared with group No. 3.

A comparison with the laboratory and field results shows that they are fairly well in agreement with the thermal conductivity of rock group No. 3. The mean value of the thermal conductivity for fresh Äspö diorite is 8 % lower and for altered Äspö diorite it is 3 % higher compared with group No. 3. Compared with the mean value from the field measurements, the measured thermal conductivity of Äspö diorite is about 7 % higher than the thermal conductivity of group No. 3.

The fine-grained granite corresponds to group No. 5. A comparison shows that as much as 22 % lower values were obtained from the field measurements. However, the extension of the fine-grained granite with the depth at this particular section (3525) is unknown and the measurements could partly have been performed in the surrounding rock, which is Äspö diorite. Thermal properties in the same order were also measured for the two rock types.

The laboratory results show that the average heat capacity of fresh Äspö diorite is 8 % higher compared with the rocks of group No. 3 and corresponding comparisons for altered Äspö diorite resulted in 5 % higher values compared with the same group. Based on the field measurements, the heat capacity is in average 7 % higher compared with the calculated heat capacity of group No. 3. The comparison is made for a density of 2750 kg/m<sup>3</sup>.

The fine-grained granite corresponds to group No. 5. The comparison shows that 8 % higher thermal conductivity values were obtained from the field measurements.

## 9.4 Possible Reasons for Differences in the Results

Reasons for the obtained differences in the results presented in Table 9-1, from the measurements as well as the calculations, can be related to:

- a) differences in properties of rock samples and of the actual rock in the field,
- b) influence of local conditions at the measurement points,
- c) performance of the tests and applied test procedures,
- d) errors in the method and limitations of background theories that the method is based on.

### a) Properties

Chemical and mineralogical properties as well as the structure of the rock have a strong influence on its thermal properties:

- chemical composition
- mineral content
- foliation
- density
- porosity
- grain size

All examined core samples representing Äspö diorite show various degrees of alterations. In some samples biotite is completely replaced by chlorite, and plagioclase by albite, epidote and sericite. From a mineralogical point of view it seems that the replacement of biotite by chlorite is responsible for the higher thermal conductivity measured in the chloritised samples. This is obvious in a plot of LOI versus thermal conductivity, Figure 9-4. The Äspö diorite samples with LOI values greater than 2 are all chloritised. The thermal conductivity of chlorite is 2-3 times higher than that of biotite.

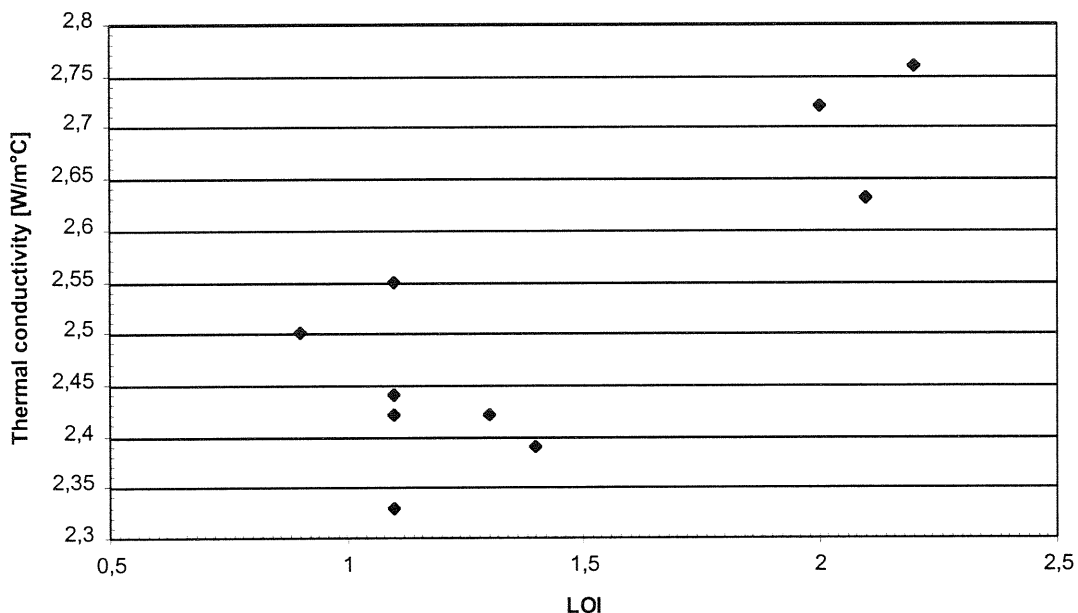


Figure 9-4 LOI content versus thermal conductivity measured in the laboratory (temperature 21 °C, saturated samples).

The results of the chemical analyses of the 19 Äspö diorite samples are largely similar. In contrast, the microscopy reveals significant variations in mineral compositions due to various degrees of alteration in the different samples.

For the evaluation of the thermal conductivity measurements, it is desirable to make comparisons with corresponding mineralogical composition of each sample. This is, however, not always possible due to factors such as the difficulty in point counting of coarse and inhomogeneous rock types. Instead, mineralogical composition, based on microscopy, and chemical data were given for fresh and altered Äspö diorite, and also for the metabasite hybride sample (called xenolith in the coremapping).

Examinations of core samples show a certain foliation parallel to the borehole axis. However, the foliation is rather weak and is therefore assumed to have a minor influence on the results.

Differences in porosity were obtained for altered and fresh Äspö diorite. The generally higher thermal conductivity of the altered Äspö diorite coincides with a higher density compared with fresh Äspö diorite. However, the variations in density and porosity among the samples are assumed to be too small to have a significant influence on the variations in the thermal properties.

Some core samples, for example sample 3569 0.87-1.20, contained large grains ( $\varnothing$  150 mm) embedded in a fine-grained mass. Laboratory measurements of thermal properties of this and other samples with a similar structure produced similar results. It may be assumed that the variations in grain size of the investigated samples did not influence the results.

Different samples were used for different types of investigations. Differences between individual samples are thus a source to uncertainties when comparing and evaluating the results. From the above discussion, it is most likely that the mineral content of different samples used in the laboratory and in the calculations, and of the actual rock in the field, account for some of the discrepancies.

#### **b) Local conditions in the field**

The field results may be influenced, to a larger or smaller degree, by different sources of error related to conditions below the ground surface (partly unknown), such as:

- water flow and high water pressures (heat convection),
- presence of joints and small fissures,
- structures of different types of rock crossing the rock mass.

Water flow during the measurements produced faulty values of the thermal properties. For example, at section 3594, the measurements were clearly disturbed by water flow in the upper part of the boreholes for the heat generating probe and temperature probe No.1. Water upflow was also observed at section 3535, in the boreholes for the heat generating probe and temperature probe No. 2. Small disturbances on the temperature curves are probably due to the influence of water.

There is a water flow into the tunnel and high water pressures have also been measured. Free water in joints and small fissures results in heat transfer due to convection. The effect is dependent on the distribution of the fissures in the rock mass.

The rock mass around the tunnel are crossed by structures of different rocks. It is sometimes difficult to estimate the extent of a certain rock type. For example, measurement in section 3566 (No. 1) resulted in a significantly higher value of the thermal conductivity compared with the other measurements in Äspö diorite. Close to this measurement point was a band of epidote which suggests that the rock may not have been homogeneous where this measurement took place.

High water pressures inside the tunnel for the Prototype Repository have previous been stated. High water flows would lead to lower measured rates of temperature increase and consequently to an overestimation of the thermal conductivity of the rock. Considering the amount of inflowing water and observations in the field, the influence on the thermal conductivity measurements of an overall water flow around the tunnel cannot be neglected. If the field results presented in Table 9-1 and 9-2 are influenced by heat convection, the influence is estimated to be at the most 10 %.

### **c) Performance of the tests and test procedures**

Parts of the actual performance of the test may influence the results. Some possible sources of error are:

- the remounting of the sensor between the measurements in the laboratory,
- compensation for the cooling process during the laboratory measurements,
- the distance between the thermal probes at the measurement depth (inclination of boreholes),
- filling of the boreholes.

The laboratory method, TPS, normally produces results with high accuracies. The measurements at room temperature 21 °C were performed by remounting the sensor between the measurements. This could have changed the position of the sensor compared with previous measurements and thereby cause unreal differences between the measurement results. However, possible changes in the position of the sensor is assumed to have a minor effect on the results.

The cooling process during the measurements at high temperatures was carefully registered. Any possible measurement errors are therefore assumed to have a negligible effect on the evaluation of the thermal properties.

In the field, the distance between the temperature probes and the heating probe can be a possible source of error. The distance was obtained from x, y and z co-ordinates at the measurement depth, 0.6 metres. Possible errors in the distance may have an influence on the thermal diffusivity and heat capacity (not the thermal conductivity). The inclination of the boreholes within the same measurement location differed in average 0.4 °, except at section 3535, where the difference amounted to 1.8 °. These differences are too small to have a significant effect on the results.

Uncompleted filling of the gap between the probes and the borehole walls is another possible source of error. The filling may also have been affected by water flow in fis-

tures. Even if the influence of unsatisfactory filling is not reflected in the measured temperature curves, it may have some minor influence on the evaluation.

From the discussion above, it appears that the filling of the boreholes may have had a minor influence on the results. However, these effects are relatively small.

#### **d) Methods and theories**

The methods used in the laboratory and in the field are based on transient conditions. Thermal properties are estimated by minimising the difference between measured and calculated temperature timeseries. This estimation is performed over a time interval for which the applied theories are valid.

The calculations use reference values, given in the literature, of thermal conductivity of different minerals. The thermal conductivity of some minerals, for example plagioclase, are known to vary significantly with chemical composition. For other minerals, the extent of such variations are not known. The calculations of the thermal conductivity resulted in large differences between fresh and altered Äspö diorite, see Table 9-1. It is possible that the thermal conductivity of the chlorite in the altered Äspö diorite differs from the reference value used. This would account for the discrepancy being much larger than observed for the fresh Äspö diorite. The calculated value of the thermal conductivity of altered Äspö diorite is assumed not to be representative.

## 10 Conclusions

If the rock mass around the Prototype Repository tunnel is subdivided in a number of major rock types, each with an estimated volume fraction and thermal conductivity, a single estimated value of the thermal conductivity can be presented using self-consistent approximation (Sundberg, 1988). An estimation of the distribution of different rock types has been made from the drill cores described in Appendix 2.

The thermal properties of the rock surrounding the Prototype Repository tunnel are estimated at:

Thermal conductivity	2.60 W/m°C
Thermal diffusivity	1.14 mm <sup>2</sup> /s
Heat capacity	2.22 MJ/m <sup>3</sup> °C (807 J/kg°C, $\rho = 2750 \text{ kg/m}^3$ )

The estimation is based on the following:

- 1) Based on the drill cores, the surrounding rock consists of 96 % Äspö diorite and 4 % xenolith. Based on available samples in this study, the Äspö diorite is 15 % fresh and 15 % altered, with the remaining 70 % somewhere between these extremes with respect to thermal properties. It should be noted that these figures are estimations founded on relatively limited data.
- 2) The thermal conductivity of altered Äspö diorite, with high chlorite content, is estimated from the laboratory measurements at 2.70 W/m°C. The thermal conductivity of fresh Äspö diorite, with a significant amount of biotite still present, is estimated at 2.32 W/m°C (mean calculated values and laboratory measurements). The thermal conductivity of medium Äspö diorite is estimated at 2.55 W/m°C (mean value of the laboratory measurements for fresh and altered Äspö diorite). The thermal conductivity of xenolith is estimated at 2.38 W/m°C, from the laboratory measurements. Using these values, a self-consistent approximation of the thermal conductivity becomes 2.53 W/m°C, but this value only considers the results from laboratory measurements and calculations.
- 3) The number of laboratory measurements is greater than the number of field measurements. Furthermore, the field values may to some degree be influenced by water flow within the rock. The thermal conductivity is therefore calculated as a weighted mean value of the field results (2.83 W/m°C) and the self-consistent approximation value based on laboratory results and calculations (2.53 W/m°C) together with weight factors 0.25 and 0.75, respectively. This way, the thermal conductivity is estimated at 2.60 W/m°C.
- 4) The thermal diffusivity is estimated from the mean value of measured values (see Figure 9-2, section 3566 excluded). The heat capacity is estimated from the mean value of calculated values (see Figure 9-3).

It should be noted that the values given above are for the rock only and so do not account for thermal transport of large water-bearing fissures.

It is estimated that the water flow in the rock mass around the Prototype Repository tunnel may have a significant effect on the evaluation of the thermal properties, especially the thermal conductivity. An internal flow introduces an additional convective heat transfer which may result in an overestimation of the thermal conductivity. The field measured values may thus overestimate the thermal conductivity of the rock mass itself.

Different alteration processes are reflected in different mineral compositions of the Äspö diorite. The replacement of biotite with chlorite in altered Äspö diorite has a significant influence on the thermal conductivity. Comparisons between fresh and altered Äspö diorite based on the laboratory measurements show that the thermal conductivity of altered Äspö diorite is on average 12 % higher than for the fresh. From a comparison of different samples within the same drill core, it is also apparent that this alteration may have taken place within very limited areas.

The discrepancies between the results from laboratory and field measurements and calculations have been discussed, and possible explanations have been suggested. Further investigations are required to reduce the uncertainties affecting the evaluation of the thermal properties.



## References

Berman R G and Brown H, 1985. Heat capacity of minerals in the system  $\text{Na}_2\text{O-K}_2\text{O-CaO-MgO-FeO-Fe}_2\text{O}_3\text{-Al}_2\text{O}_3\text{-SiO}_2\text{-TiO}_2\text{-H}_2\text{O-CO}_2$ : representation, estimation, and high temperature extrapolation. *Contrib. Mineral Petrol.*, 89, p 163-183.

Gustafsson S, 1991. Transient plane source techniques for thermal conductivity and thermal diffusivity measurements of solid materials. *Rev. Sci. Instrum.* 62, p 797-804. American Institute of Physics, USA.

Horai K, 1971. Thermal conductivity of rock-forming minerals. *J. Geophys. Res.* 76, p 1278-1308.

Horai K and Simmons G, 1969. Thermal conductivity of rock-forming minerals. *Earth Planet. Sci. Lett.*, 6, p 359-368.

Patel S, Dahlström L-O, Stenberg L, 1997. Characterisation of the rock mass in the Prototype Repository at Äspö HRL, Stage 1. SKB HRL, Progress Report HRL-97-24. Stockholm, Sweden.

Sibbit W L, Dodson J G and Tester J W, 1979. Thermal conductivity of crystalline rocks associated with energy extraction from hot dry rock geothermal systems. *J. Geophys. Res.*, 71, p 12.

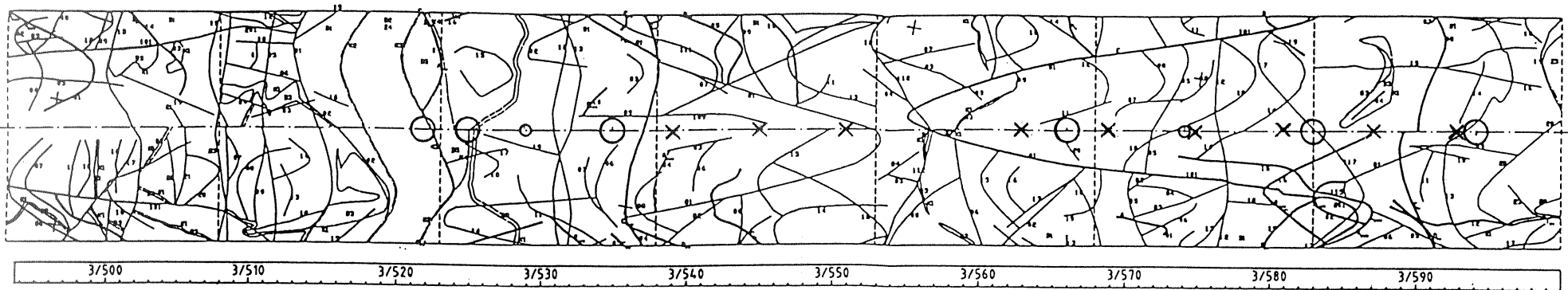
Sundberg J and Gabrielsson A, 1998. Field measurements of thermal properties of the rocks in the prototype repository at Äspö HRL. SKB HRL, Progress Report HRL-98-28. Stockholm, Sweden.

Sundberg J, 1991:1. Thermal properties of the rocks on Äspö island. Thermal conductivity, heat capacity, geothermal gradient and heat flow. SKB HRL, Progress Report 25-91-09. Stockholm, Sweden.

Sundberg J, 1991:2. Thermal properties in soils and rocks, Information 12. (In Swedish). Swedish Geotechnical Institute, Linköping, Sweden.

Sundberg J, 1988. Thermal properties of soils and rocks, Publ. A 57 Dissertation. Department of Geology, Chalmers University of Technology and University of Göteborg, Sweden.

## **Appendix 1: Position of field measurements and core drillings for laboratory measurements**



- Thermal probe measurement
- Reference temperature
- × Core drilling

## **Appendix 2: Rock Classification of Drill Cores**

SITE	IDCODE	FROM_LENGTH	TO_LENGTH	ROCK	ROCKNAME	LENGTH
ÄSPÖ	KA3539G	0,000	7,46	PSF	ÄSPÖ DIORITE	7,460
ÄSPÖ	KA3545G	0,000	7,48	PSF	ÄSPÖ DIORITE	7,480
ÄSPÖ	KA3551G	0,000	7,45	PSF	ÄSPÖ DIORITE	7,450
ÄSPÖ	KA3563G	0,001	7,45	PSF	ÄSPÖ DIORITE	7,449
ÄSPÖ	KA3569G	0,001	7,47	PSF	ÄSPÖ DIORITE	7,469
ÄSPÖ	KA3575G	0,002	7,46	PSF	ÄSPÖ DIORITE	7,458
ÄSPÖ	KA3581G	0,002	7,47	PSF	ÄSPÖ DIORITE	7,468
ÄSPÖ	KA3587G	0,002	7,48	PSF	ÄSPÖ DIORITE	7,478
ÄSPÖ	KA3593G	0,000	7,55	PSF	ÄSPÖ DIORITE	7,550
				SUM		67,262 METRES

SITE	IDCODE	FROM_LENGTH	TO_LENGTH	VEIN	VEIN NAME	LENGTH	XEN	HSB	PSE
ÄSPÖ	KA3539G	1,17	1,24	XEN	XENOLITH	0,07	0,07		
ÄSPÖ	KA3539G	3,48	3,53	XEN	XENOLITH	0,05	0,05		
ÄSPÖ	KA3545G	3,20	3,23	HSB	PEGMATITE	0,03		0,03	
ÄSPÖ	KA3545G	3,51	3,60	XEN	XENOLITH	0,09	0,09		
ÄSPÖ	KA3545G	5,60	5,64	XEN	XENOLITH	0,04	0,04		
ÄSPÖ	KA3545G	5,97	5,97	XEN	XENOLITH	0	0		
ÄSPÖ	KA3545G	6,50	6,56	XEN	XENOLITH	0,06	0,06		
ÄSPÖ	KA3551G	1,95	2,05	XEN	XENOLITH	0,1	0,1		
ÄSPÖ	KA3551G	4,57	4,73	XEN	XENOLITH	<b>0,16</b>	0,16		
ÄSPÖ	KA3551G	5,76	5,78	XEN	XENOLITH	0,02	0,02		
ÄSPÖ	KA3563G	0,04	0,08	XEN	XENOLITH	0,046	0,046		
ÄSPÖ	KA3563G	3,25	3,36	XEN	XENOLITH	<b>0,11</b>	0,11		
ÄSPÖ	KA3563G	4,94	4,97	XEN	XENOLITH	0,03	0,03		
ÄSPÖ	KA3569G	1,12	1,17	HSB	PEGMATITE	0,05		0,05	
ÄSPÖ	KA3569G	3,62	3,70	XEN	XENOLITH	0,08	0,08		
ÄSPÖ	KA3569G	3,82	3,93	XEN	XENOLITH	<b>0,11</b>	0,11		
ÄSPÖ	KA3569G	4,57	4,59	HSB	PEGMATITE	0,02		0,02	
ÄSPÖ	KA3575G	0,17	0,19	XEN	XENOLITH	0,016	0,016		
ÄSPÖ	KA3575G	4,01	4,07	XEN	XENOLITH	0,06	0,06		
ÄSPÖ	KA3575G	5,56	5,61	XEN	XENOLITH	0,05	0,05		
ÄSPÖ	KA3581G	0,18	0,23	XEN	XENOLITH	0,056	0,056		
ÄSPÖ	KA3581G	0,89	1,09	XEN	XENOLITH	<b>0,201</b>	0,201		
ÄSPÖ	KA3581G	1,17	1,23	XEN	XENOLITH	0,06	0,06		
ÄSPÖ	KA3581G	1,43	1,49	XEN	XENOLITH	0,06	0,06		
ÄSPÖ	KA3581G	2,13	2,18	XEN	XENOLITH	0,05	0,05		
ÄSPÖ	KA3581G	2,58	2,65	XEN	XENOLITH	0,07	0,07		
ÄSPÖ	KA3581G	3,77	3,81	XEN	XENOLITH	0,04	0,04		
ÄSPÖ	KA3581G	6,80	6,94	XEN	XENOLITH	<b>0,14</b>	0,14		
ÄSPÖ	KA3581G	7,02	7,40	PSE	SMÅLAND GRANITE	<b>0,38</b>			0,38
ÄSPÖ	KA3587G	1,37	1,41	XEN	XENOLITH	0,04	0,04		
ÄSPÖ	KA3587G	2,90	2,92	HSB	PEGMATITE	0,02		0,02	
ÄSPÖ	KA3587G	5,46	5,50	XEN	XENOLITH	0,04	0,04		
ÄSPÖ	KA3587G	6,52	6,70	HSB	PEGMATITE	<b>0,18</b>		0,18	
ÄSPÖ	KA3593G	0,87	0,94	XEN	XENOLITH	0,071	0,071		
ÄSPÖ	KA3593G	2,08	2,13	XEN	XENOLITH	0,05	0,05		
ÄSPÖ	KA3593G	2,67	2,96	XEN	XENOLITH	<b>0,29</b>	0,29		
ÄSPÖ	KA3593G	4,15	4,37	XEN	XENOLITH	<b>0,22</b>	0,22		
ÄSPÖ	KA3593G	5,27	5,56	XEN	XENOLITH	<b>0,29</b>	0,29		
ÄSPÖ	KA3593G	6,15	6,22	XEN	XENOLITH	0,07	0,07		
ÄSPÖ	KA3593G	6,72	6,73	HSB	PEGMATITE	0,01		0,01	
						3,53	2,84	0,31	0,38
					SHARE OF CORE	0,052	0,042	0,005	0,006

## **Appendix 3: Density and water absorption of core samples**

Sample	diameterxheight (c. mm)	Weight loss* (gm)	Density (kg/m <sup>3</sup> )	Water absorption before		Water absorption after 15 h		Water absorption before		Water absorption after 15 h	
				boiling, excl weight loss. (weight %)	(volumetric %)	of boiling, excl weight loss. (weight %)	(volumetric %)	boiling, incl weight loss. (weight %)	(volumetric %)	of boiling, incl weight loss. (weight %)	(volumetric %)
KA3539-1 1.0-1.22	45,0x107,9	0,03	2769	0,13	0,36	0,13	0,35	0,14	0,39	0,14	0,38
KA3539-2 5.50-5.68	45,1x63,1	0,07	2716	0,1	0,28	0,1	0,27	0,13	0,36	0,13	0,34
KA3545 0.83-1.11	45,1x89,5	0,03	2733	0,11	0,3	0,11	0,3	0,12	0,32	0,12	0,32
KA3551 0.95-1.15	45,0x46,9	0,05	2713	0,14	0,37	0,14	0,37	0,16	0,45	0,16	0,45
KA3551 0.95-1.15	45,0x55,5	0,03	2734	0,11	0,31	0,11	0,3	0,13	0,35	0,12	0,33
KA3563 0.88-1.12	44,9x71,6	0,1	2745	0,13	0,36	0,13	0,36	0,17	0,47	0,17	0,47
KA3569 0.87-1.20	45,0x74,6	0,07	2740	0,08	0,23	0,07	0,19	0,11	0,3	0,1	0,27
KA3569 0.87-1.20	45,1x68,7	0,05	2750	0,1	0,27	0,09	0,24	0,12	0,33	0,11	0,29
KA3575 1.03-1.27	45,0x75,7	0,05	2764	0,1	0,28	0,1	0,27	0,12	0,32	0,11	0,32
KA3581 1.10-1.33	45,0x54,2	0,05	2815	0,1	0,28	0,09	0,27	0,12	0,34	0,12	0,33
KA3581 1.10-1.33	45,0x15,5	0,03	2724	0,14	0,39	0,14	0,39	0,21	0,56	0,21	0,56
KA3587 0.97-1.14	45,0x54,7	0,05	2777	0,1	0,26	0,09	0,25	0,12	0,32	0,11	0,31
KA3593-1 1.42-1.63	45,0x66,1	0,06	2736	0,14	0,38	0,13	0,37	0,17	0,45	0,16	0,44
KA3593-1 1.42-1.63	45,0x13,0	0,03	2748	0,17	0,46	0,17	0,46	0,23	0,64	0,23	0,64
KA3593-2 4.19-4.43 (xenolith)	45,0x56,0	0	2820	0,22	0,62	0,22	0,62	0,22	0,62	0,22	0,62
Mean ÄD		0,050	2747,4	0,12	0,32	0,11	0,31	0,15	0,40	0,14	0,39
Min ÄD		0,03	2713	0,08	0,23	0,07	0,19	0,11	0,3	0,1	0,27
Max ÄD		0,1	2815	0,17	0,46	0,17	0,46	0,23	0,64	0,23	0,64
Standard deviation ÄD		0,020	27,018	0,024	0,064	0,027	0,072	0,037	0,102	0,039	0,109

\*) Weight loss after water storage and boiling.



## **Appendix 4: Chemical data of core samples**

Sample	SiO2	Al2O3	CaO	Fe2O3	K2O	MgO	MnO2	Na2O	P2O5	TiO2	LOI	Ba	Nb	Sr	Y	Zr
Ka3539 1.0-1.22	59,5	18	4,62	5,7	2,85	2,44	0,122	5,06	0,352	0,885	1,1	1330	32,4	1320	25,9	259
KA3539 5.50-5.68	58,4	17,3	3,33	6,32	4,74	3,06	0,132	3,76	0,36	0,911	2,1	1600	39	1070	25,3	268
KA3539 7.0-7.17	56,5	17,2	4,48	7,31	2,55	3,28	0,148	4,22	0,464	1,03	2,2	1470	36,8	1180	26,6	216
KA3545 0.83-1.11	59,1	17,5	4,49	6,28	3,39	2,73	0,119	3,97	0,353	0,926	2	1420	36,7	1340	27,5	262
KA3545 6.99-7.10	59,8	17,8	4,19	5,78	3,18	2,46	0,114	4,44	0,358	0,898	1,7	1550	33,1	1280	26,8	242
KA 3551 0.95-1.15	57,9	17,6	4,07	6,14	3,85	2,87	0,126	3,92	0,364	0,914	2,2	1520	33,2	1330	28,6	259
KA3551 6.90-7.05	59,5	17,7	4,57	5,93	2,27	2,77	0,119	5,13	0,351	0,878	1,7	1220	27,5	1280	24,5	256
KA3563 0.88-1.12	60	17,4	4,89	5,6	3,14	2,37	0,104	4,38	0,342	0,845	1,4	1580	31,2	1290	23,2	248
KA3563 6.97-7.11	58,2	18	4,85	6,37	3,2	2,67	0,116	4,72	0,371	0,939	1,1	1460	33,7	1350	24,8	293
KA3569 0.87-1.20	61,6	17	3,92	4,9	4,1	2,05	0,102	4,38	0,301	0,752	1,3	2490	26,1	1200	21,9	204
KA3569 6.88-7.02	59,1	17,6	5,03	5,58	2,58	2,29	0,115	5,33	0,339	0,829	1,5	959	30,6	1190	23	229
KA3575 1.03-1.27	60,4	17,4	4,26	5,34	3,28	2,18	0,0943	4,67	0,321	0,77	1,1	1760	29,9	1310	22,3	236
KA3575 6.98-7.12	59,9	17,8	4,86	5,87	3,22	2,44	0,106	4,61	0,364	0,897	0,8	1680	31,4	1390	23,6	238
KA3581 1.10-1.33	59,1	17,4	4,66	6,17	3,37	2,75	0,113	4,44	0,386	0,927	0,9	1830	30,3	1310	25	278
Ka3581 6.80-6.95	59,5	17,7	4,7	5,77	3,07	2,43	0,107	4,75	0,349	0,906	0,8	1590	32,1	1280	28,6	251
KA3587 0.97-1.14	59,1	18,1	4,76	5,98	3,28	2,52	0,115	4,68	0,362	0,866	1,1	1670	32,6	1390	24	249
KA3587 7.12-7.25	59	18,1	4,93	5,97	3	2,49	0,118	4,85	0,369	0,903	1,1	1370	29,5	1310	25,8	247
KA3593 1.42-1.63	60,6	17,5	4,28	5,43	3,43	2,3	0,0999	4,56	0,334	0,827	1,1	1790	27,4	1240	24,9	233
KA3593 4.19-4.43	50,9	16,4	7,08	9,43	2,59	5,22	0,215	3,4	0,734	1,59	2,7	707	40,2	1200	41,1	317
KA3593 6.93-7.12	59,5	17,3	4,69	6,48	3,2	2,79	0,117	4,47	0,419	0,994	1	1330	31,4	1280	30,3	242
Redstained ÄD	SiO2	Al2O3	CaO	Fe2O3	K2O	MgO	MnO2	Na2O	P2O5	TiO2	LOI	Ba	Nb	Sr	Y	Zr
KA3539 5.50-5.68	58,4	17,3	3,33	6,32	4,74	3,06	0,132	3,76	0,36	0,911	2,1	1600	39	1070	25,3	268
KA3545 0.83-1.11	59,1	17,5	4,49	6,28	3,39	2,73	0,119	3,97	0,353	0,926	2	1420	36,7	1340	27,5	262
KA 3551 0.95-1.15	57,9	17,6	4,07	6,14	3,85	2,87	0,126	3,92	0,364	0,914	2,2	1520	33,2	1330	28,6	259
<b>Mean value</b>	<b>58,5</b>	<b>17,5</b>	<b>3,96</b>	<b>6,24</b>	<b>3,99</b>	<b>2,89</b>	<b>0,126</b>	<b>3,88</b>	<b>0,359</b>	<b>0,917</b>	<b>2,1</b>	<b>1513</b>	<b>36,3</b>	<b>1247</b>	<b>27,1</b>	<b>263</b>
Fresh ÄD	SiO2	Al2O3	CaO	Fe2O3	K2O	MgO	MnO2	Na2O	P2O5	TiO2	LOI	Ba	Nb	Sr	Y	Zr
KA3563 0.88-1.12	60	17,4	4,89	5,6	3,14	2,37	0,104	4,38	0,342	0,845	1,4	1580	31,2	1290	23,2	248
KA3587 0.97-1.14	59,1	18,1	4,76	5,98	3,28	2,52	0,115	4,68	0,362	0,866	1,1	1670	32,6	1390	24	249
<b>Mean value</b>	<b>59,5</b>	<b>17,7</b>	<b>4,82</b>	<b>5,79</b>	<b>3,21</b>	<b>2,44</b>	<b>0,1</b>	<b>4,53</b>	<b>0,352</b>	<b>0,856</b>	<b>1,25</b>	<b>1625</b>	<b>31,7</b>	<b>1340</b>	<b>23,6</b>	<b>248</b>

## **Appendix 5: Thermal properties in the laboratory**

Thermal properties measured in the laboratory  
Äspö diorite and xenolith

Temperature 21 °C

Sample	Thermal conductivity (W/m°C)		Thermal diffusivity (mm <sup>2</sup> /s)		Heat capacity (MJ/m <sup>3</sup> °C)	
	dry	saturated	dry	saturated	dry	saturated
3539-1 1.0-1.22	2,37	2,42	1,09	1,09	2,17	2,22
3539-2 5.50-5.68	2,41	2,63	1,08	1,23	2,23	2,14
3545 0.83-1.11	2,63	2,72	1,17	1,2	2,25	2,27
3551 0.95-1.15	2,66	2,76	1,22	1,29	2,18	2,15
3563 0.88-1.12	2,37	2,39	1,13	1,11	2,1	2,15
3569 0.87-1.20	2,41	2,42	1,14	1,11	2,12	2,19
3575 1.03-1.27	2,43	2,44	1,15	1,12	2,12	2,18
3581 1.10-1.33	2,43	2,5	1,09	1,08	2,24	2,32
3587 0.97-1.14	2,35	2,33	1,08	1,02	2,18	2,29
3593-1 1.42-1.63	2,54	2,55	1,26	1,21	2,01	2,1
3593-2 4.19-4.43 (xenolith)	2,61	2,38	1,24	1,02	2,1	2,33
Mean Äspö diorite (10 samples)	2,46	2,52	1,14	1,15	2,16	2,20

SAMPLE 3587

Temperature (°C)	Thermal con (W/m°C)	Thermal diff. (mm <sup>2</sup> /s)	Heat cap. (MJ/m <sup>3</sup> °C)
0	2,309	1,086	2,126
21	2,33	1,02	2,29
45,4	2,363	1,018	2,321
46,7	2,362	0,9967	2,37
47,9	2,365	1,014	2,331
48,8	2,36	0,9785	2,412
49,9	2,355	0,9928	2,372
64,3	2,36	1,01	2,336
66,7	2,346	0,9831	2,387
69,3	2,352	0,9639	2,44
72,5	2,333	0,9835	2,372
75,5	2,322	0,9395	2,471
78	2,335	0,8383	2,786

SAMPLE 3575

Temperature (°C)	Thermal con (W/m°C)	Thermal diff. (mm <sup>2</sup> /s)	Heat cap. (MJ/m <sup>3</sup> °C)
0	2,469	1,272	1,941
21	2,44	1,12	2,18
41,7	2,465	1,135	2,173
46,6	2,475	1,139	2,173
47,7	2,474	1,126	2,198
58,2	2,475	1,104	2,241
64,3	2,453	1,073	2,287
71,8	2,455	1,078	2,276
74,3	2,461	1,031	2,387
77,4	2,456	1,02	2,408

SAMPLE 3563

Temperature (°C)	Thermal con (W/m°C)	Thermal diff. (mm <sup>2</sup> /s)	Heat cap. (MJ/m <sup>3</sup> °C)
0	2,353	1,194	1,971
21	2,39	1,11	2,15
49,7	2,355	1,002	2,35
52,8	2,381	1,054	2,259
54,3	2,359	1,034	2,282
71,7	2,379	1,038	2,291
74,4	2,361	0,9913	2,382
77,1	2,396	1,004	2,388

SAMPLE 3545

Temperature (°C)	Thermal con (W/m°C)	Thermal diff. (mm <sup>2</sup> /s)	Heat cap. (MJ/m <sup>3</sup> °C)
0	2,644	1,292	2,046
21	2,72	1,2	2,27
51,4	2,635	1,121	2,35
53,7	2,637	1,139	2,315
54,7	2,642	1,145	2,306
57,2	2,638	1,103	2,392
72,6	2,628	1,064	2,471
75,5	2,617	1,076	2,432
78,5	2,655	1,122	2,365

## **Appendix 6: Co-ordinates of boreholes and layout at the thermal probe measurement points**

**SKB Äspö HRL**

Positioning of boreholes.

Measured 1998/02/17 13:44-15:35 by

Johannes Heikkilä

Co-ordinate system: Äspö 1996

IDCODE	DEPTH (m)	X North	Y East	Z Dip	DECLIN (°)	INCLIN (DOWN) (°)	DIST. TO HEAT PROBE (m)	DIST. TO REF. (m)	IDCODE REF. TEMP.
PA3522G01 (TEMP. PROB NO. 1)	0,0 0,6	7265,748 7265,741	1943,187 1943,181	-449,419 -450,019	219,8	-89,1	0,17028 0,16609	6,89 6,90	PA3529G01
PA3522G02 (HEAT PROBE	0,0 0,6	7265,670 7265,663	1943,038 1943,037	-449,394 -449,994	189,5	-89,3		6,76 6,77	PA3529G01
PA3522G03 (TEMP. PROB NO. 2)	0,0 0,6	7265,812 7265,801	1942,961 1942,959	-449,421 -450,021	186,3	-89,0	0,16338 0,16030	6,66 6,67	PA3529G01
PA3525G01	0,0 0,6	7267,452 7267,442	1939,857 1939,853	-449,335 -449,935	206,6	-89,0	0,15197 0,15986	3,53 3,55	PA3529G01
PA3525G02	0,0 0,6	7267,469 7267,465	1940,008 1940,011	-449,329 -449,929	146,3	-89,6		3,68 3,71	PA3529G01
PA3525G03	0,0 0,6	7267,328 7267,325	1940,020 1940,018	-449,363 -449,963	213,7	-89,6	0,14489 0,14456	3,67 3,69	PA3529G01
PA3535G01	0,0 0,6	7268,346 7268,349	1930,374 1930,371	-449,212 -449,812	303,7	-89,6	0,15949 0,14852	6,20 6,19	PA3529G01
PA3535G02	0,0 0,6	7268,502 7268,494	1930,402 1930,388	-449,190 -449,790	243,4	-88,5		6,21 6,21	PA3529G01
PA3535G03	0,0 0,6	7268,476 7268,464	1930,558 1930,538	-449,194 -449,793	238,0	-87,8	0,15742 0,15357	6,05 6,06	PA3529G01
PA3566G01	0,0 0,6	7272,688 7272,689	1899,271 1899,270	-448,596 -449,196	315,0	-89,8	0,16125 0,16039	7,42 7,43	PA3574G01
PA3566G02	0,0 0,6	7272,800 7272,803	1899,387 1899,383	-448,590 -449,190	303,7	-89,6		7,51 7,53	PA3574G01
PA3566G03	0,0 0,6	7272,687 7272,692	1899,498 1899,492	-448,598 -449,198	308,7	-89,3	0,15897 0,15556	7,64 7,65	PA3574G01

IDCODE	DEPTH (m)	X North	Y East	Z Dip	DECLIN (°)	INCLIN (DOWN) (°)	DIST. TO HEAT PROBE (m)	DIST. TO REF. (m)	IDCODE REF. TEMP
PA3583G01	0,0	7274,540	1882,966	-448,240	315,0	-89,7	0,16620	9,01	PA3574G01
	0,6	7274,542	1882,964	-448,840			0,16818	8,99	
PA3583G02	0,0	7274,441	1882,835	-448,216	206,6	-89,7		9,13	PA3574G01
	0,6	7274,438	1882,834	-448,816				9,11	
PA3583G03	0,0	7274,566	1882,738	-448,233	180,0	-89,8	0,15965	9,24	PA3574G01
	0,6	7274,564	1882,738	-448,833			0,15893	9,22	
PA3594G01	0,0	7276,033	1871,763	-447,984	34,8	-83,6	0,16283	20,31	PA3574G01
	0,6	7276,088	1871,802	-448,580			0,16504	20,26	
PA3594G02	0,0	7276,119	1871,625	-447,996	32,9	-83,0		20,45	PA3574G01
	0,6	7276,180	1871,665	-448,591				20,40	
PA3594G03	0,0	7276,268	1871,707	-448,017	30,3	-83,6	0,17153	20,39	PA3574G01
	0,6	7276,325	1871,741	-448,614			0,16565	20,34	
PA3574G01	0,0	7273,762	1891,935	-448,475	337,8	-86,7			
	0,6	7273,794	1891,922	-449,074					
PA3529G01	0,0	7266,832	1936,382	-449,293	208,3	-86,6			
	0,6	7266,801	1936,365	-449,892					

### Layout of boreholes for thermal probe measurements

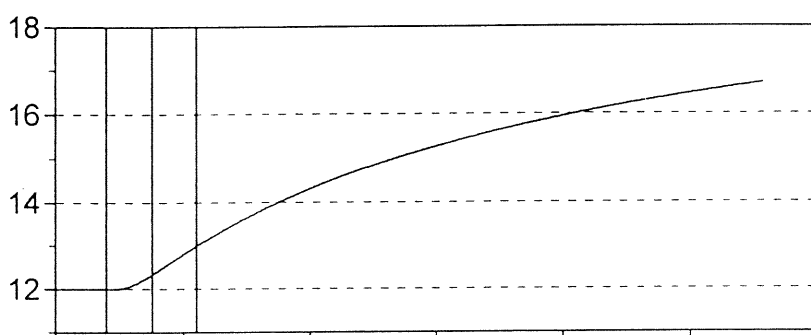
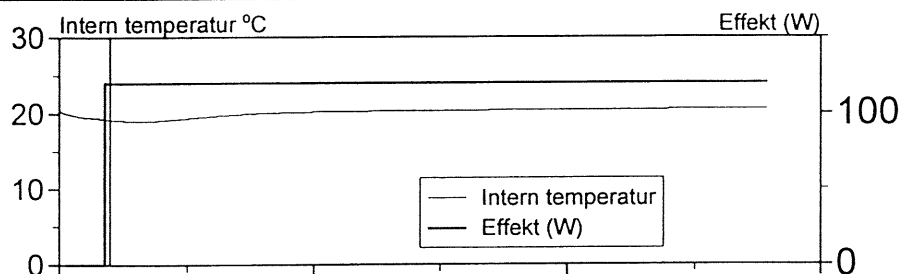
----- bottom of the tunnel  
 —————> direction of the end of the tunnel (westward)

Section	
3522	<p>PA3522G03 ●</p> <p>PA3522G02 ●</p> <p>PA3522G01 ●</p>
3525	<p>PA3525G01 ●</p> <p>PA3525G02 ●</p> <p>PA3525G03 ●</p>
3535	<p>PA3535G01 ● PA3535G02 ●</p> <p>PA3535G03 ●</p>
3566	<p>PA3566G01 ●</p> <p>PA3566G02 ●</p> <p>PA3566G03 ●</p>
3583	<p>PA3583G03 ●</p> <p>PA3583G02 ●</p> <p>PA3583G01 ●</p>
3594	<p>PA3594G02 ●</p> <p>PA3594G03 ●</p> <p>PA3594G01 ●</p>



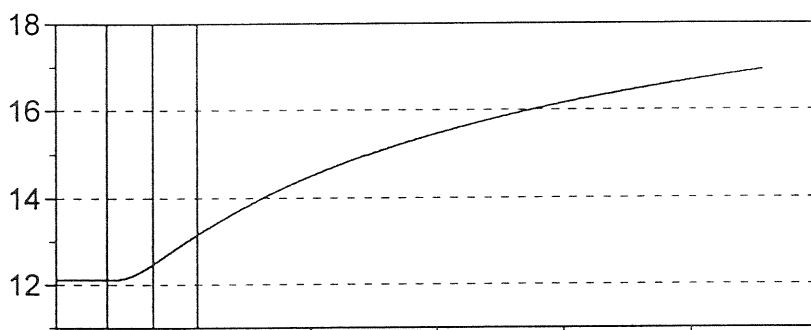
## **Appendix 7: Data and Graphic Presentations of Results from Thermal Probe Measurements**

Projekt	Prototypförvaret - Äspö	Längd	1.20 m
Projektnummer	2-9709-451	Diameter	13 mm
Datum	98-01-21	Max effekt	120 W
Plats	Tunnel, 450 m djup	Max temperatur	100 grader
Sektion	3522 vänster	Värmspiralens resistans	7.2 ohm
Material	Mylonitgång	Värmspiralens längd	1200 mm
Provdjup	0,6 m		
Operatör	MB/AG		



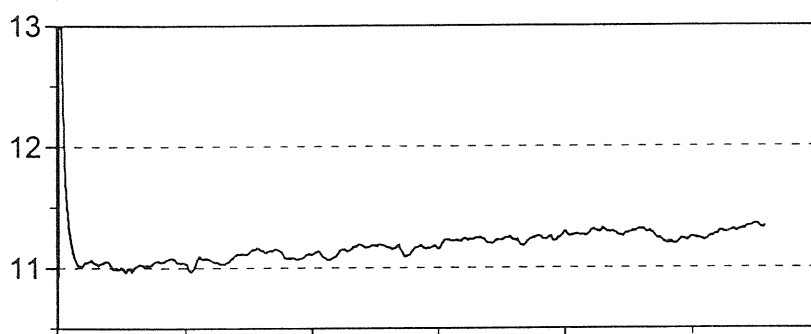
### Temperatursond 1

Placering	Parallellt mylonitgång
Avstånd	0.166 m
Starttemperatur	12.00 °C
Värmeledningsförmåga	3.16 W/m°C
Värmediffusivitet	1.444E-06 m <sup>2</sup> /s
Värmekapacitet	0.61 kWh/m <sup>3</sup> °C
Standardavvikelse	0.000 °C



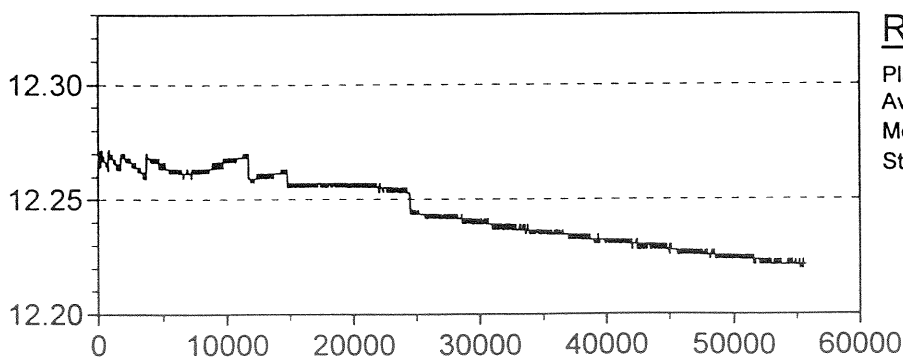
### Temperatursond 2

Placering	Vinkelrät mylonitgång
Avstånd	0.160 m
Starttemperatur	12.12 °C
Värmeledningsförmåga	3.16 W/m°C
Värmediffusivitet	1.387E-06 m <sup>2</sup> /s
Värmekapacitet	0.63 kWh/m <sup>3</sup> °C
Standardavvikelse	0.000 °C



### Temperatursond 3

Placering	Används inte
Avstånd	0.000 m
Starttemperatur	10.92 °C
Värmeledningsförmåga	0.00 W/m°C
Värmediffusivitet	0.000E+00 m <sup>2</sup> /s
Värmekapacitet	0.00 kWh/m <sup>3</sup> °C
Standardavvikelse	0.000 °C



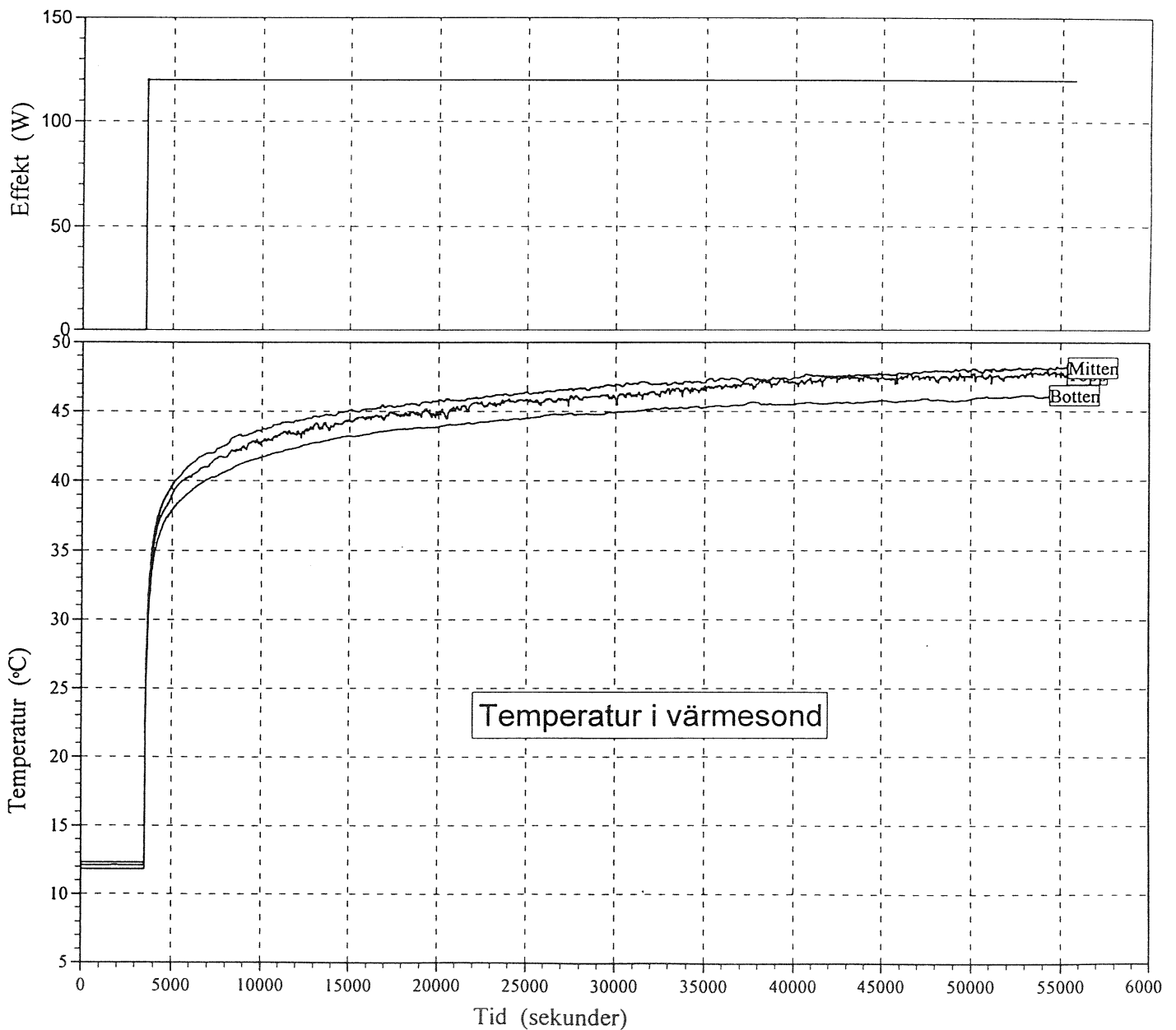
### Referenstemperatur

Placering	Referenstemperatur
Avstånd	6.8 m
Medeltemperatur	12.24 °C
Standardavvikelse	0.0149 °C

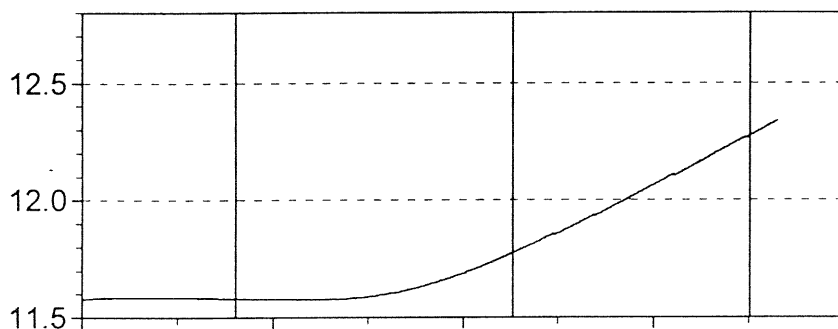
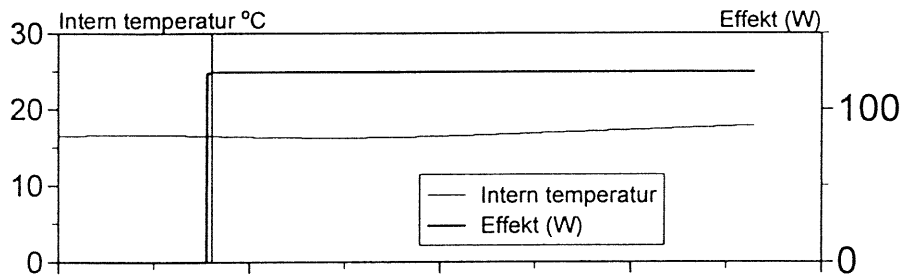
## ENERGI

## TERMISKA EGENSKAPER

Prototypförvaret - Äspö Tunnel, 450 m djup			Datum 1998-10-15		
			Projektnummer 2-9709-451		
Sektion 3522 vänster	Provdjup 0,6 m	Material Mylonitgång	Signatur		
Försöksdatum 98-01-21	Filnamn 3522-4B.TSW	Utfört av MB/AG			
Referenstemperatur 12.24 °C	Effekt 119.98 W 99.98 W/m	Beräkningsresultat			
Standardavvikelse 0.015 °C	Standardavvikelse 0.0214 W	Temperatursond	1	2	3
		Avstånd	0.166	0.160	0.000 m
		Värmeledningsförmåga	3.16	3.16	0.00 W/m°C
		Värmediffusivitet	1.44E-06	1.39E-06	0.00E+00 m <sup>2</sup> /s
		Värmekapacitet	0.61	0.63	0.00 kWh/m <sup>3</sup> °C

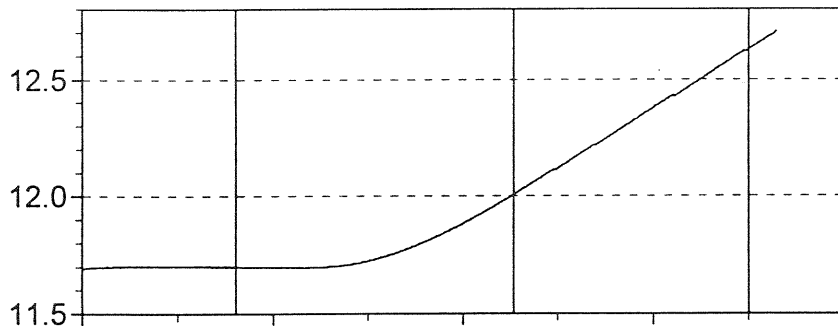


Projekt	Prototypförvaret - Äspö	Längd	1.20 m
Projektnummer	2-9709-451	Diameter	13 mm
Datum	98-01-29	Max effekt	120 W
Plats	Tunnel	Max temperatur	100 grader
Sektion	3525 höger	Värmspiralens resistans	7.2 ohm
Material	Finkornig granit (röd)	Värmspiralens längd	1200 mm
Provdjup	0.6 m		
Operatör	MB/AG		



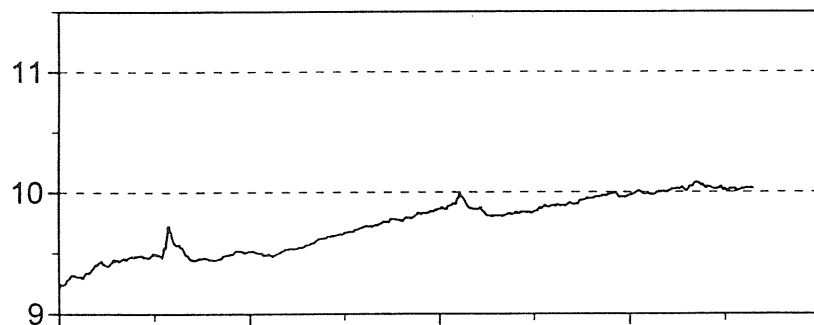
### Temperatursond 1

Placering	I mindre lokal (d ca 0,3 m)
Avstånd	0.160 m
Starttemperatur	11.58 °C
Värmeledningsförmåga	2.72 W/m°C
Värmediffusivitet	1.216E-06 m <sup>2</sup> /s
Värmekapacitet	0.62 kWh/m <sup>3</sup> °C
Standardavvikelse	0.000 °C



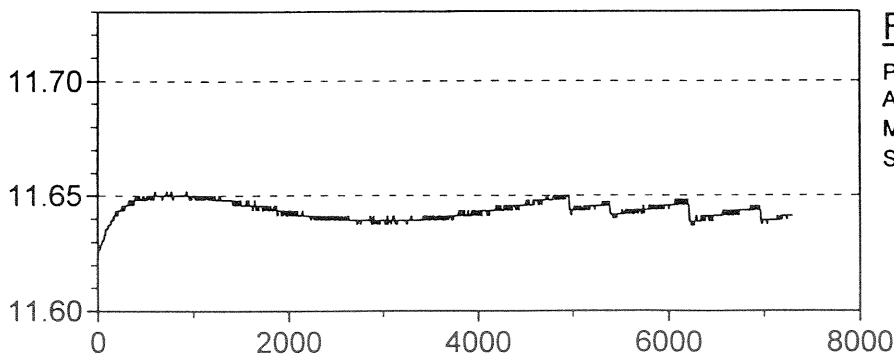
### Temperatursond 2

Placering	I mindre lokal (d ca 0,3 m)
Avstånd	0.145 m
Starttemperatur	11.70 °C
Värmeledningsförmåga	2.71 W/m°C
Värmediffusivitet	1.205E-06 m <sup>2</sup> /s
Värmekapacitet	0.62 kWh/m <sup>3</sup> °C
Standardavvikelse	0.000 °C



### Temperatursond 3

Placering	Används inte
Avstånd	0.000 m
Starttemperatur	9.22 °C
Värmeledningsförmåga	0.00 W/m°C
Värmediffusivitet	0.000E+00 m <sup>2</sup> /s
Värmekapacitet	0.00 kWh/m <sup>3</sup> °C
Standardavvikelse	0.000 °C



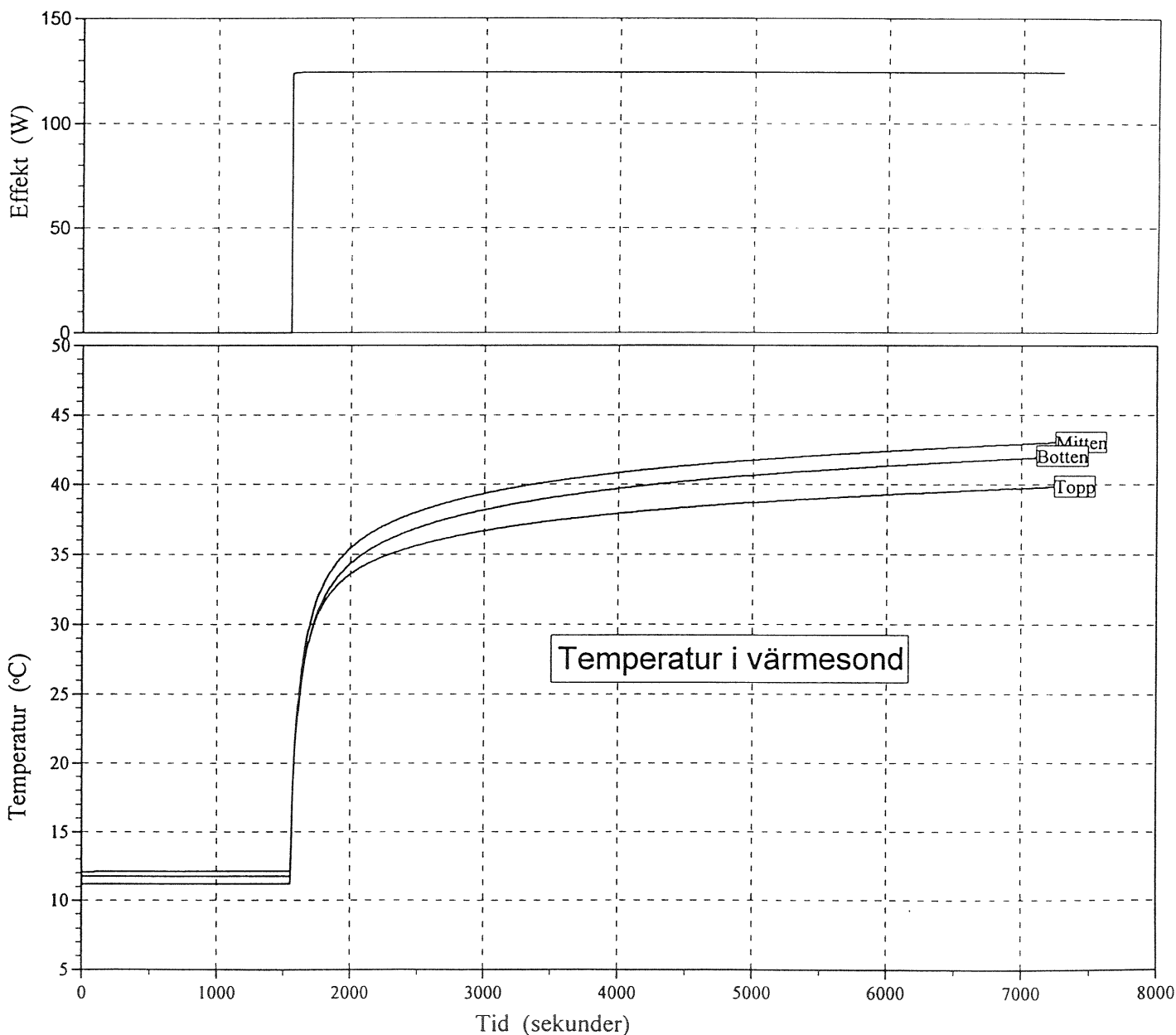
### Referenstemperatur

Placering	Referenstemperatur
Avstånd	3.7 m
Medeltemperatur	11.64 °C
Standardavvikelse	0.0029 °C

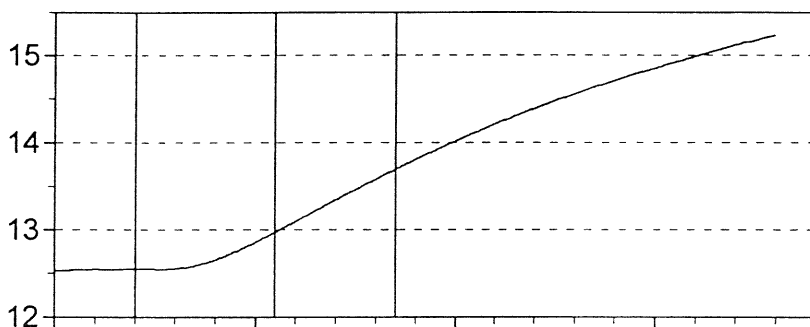
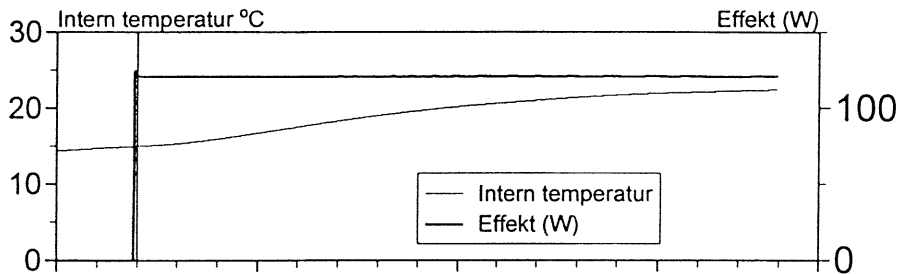
## ENERGI

## TERMISKA EGENSKAPER

Prototypförvaret - Äspö Tunnel			Datum	1998-10-15	
			Projektnummer	2-9709-451	
Sektion	Provdjup	Material	Signatur		
3525 höger	0,6 m	Finkornig granit (röd)			
Försöksdatum	Filnamn	Utfört av			
98-01-29	3525-5A.TSW	MB/AG			
Referenstemperatur	Effekt	Beräkningsresultat			
11.64 °C	124.49 W 103.75 W/m	Temperatursond	1	2	3
Standardavvikelse	Standardavvikelse	Avstånd	0.160	0.145	0.000 m
0.003 °C	0.0352 W	Värmeledningsförmåga	2.72	2.71	0.00 W/m°C
		Värmediffusivitet	1.22E-06	1.20E-06	0.00E+00 m <sup>2</sup> /s
		Värme kapacitet	0.62	0.62	0.00 kWh/m <sup>3</sup> °C

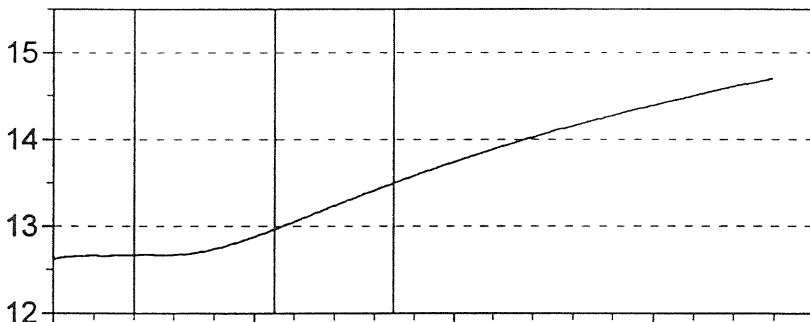


Projekt	Prototypförvaret - Äspö	Längd	1.20 m
Projektnummer	2-9709-451	Diameter	13 mm
Datum	98-01-21	Max effekt	120 W
Plats	Tunnel, 450 m djup	Max temperatur	100 grader
Sektion	3535 höger (måtn.nr1)	Värmspiralens resistans	7.2 ohm
Material	Homogen Äspödiorit	Värmspiralens längd	1200 mm
Provdjup	0,6 m		
Operatör	MB/AG		



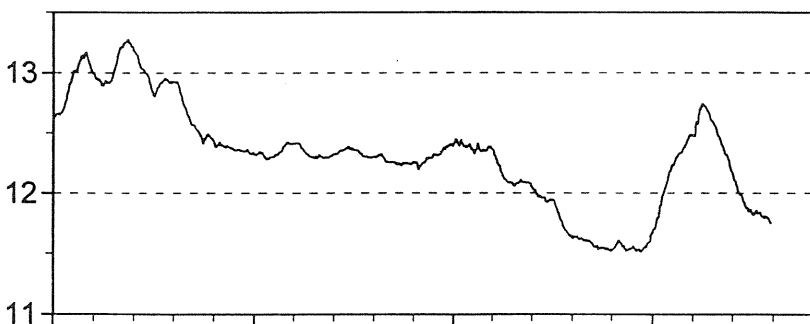
### Temperatursond 1

Placering V-rät tunnel, lite vatten fr värnehål  
 Avstånd 0.149 m  
 Starttemperatur 12.55 °C  
 Värmeledningsförmåga 2.73 W/m°C  
 Värmediffusivitet 1.268E-06 m<sup>2</sup>/s  
 Värmekapacitet 0.60 kWh/m<sup>3</sup>°C  
 Standardavvikelse 0.000 °C



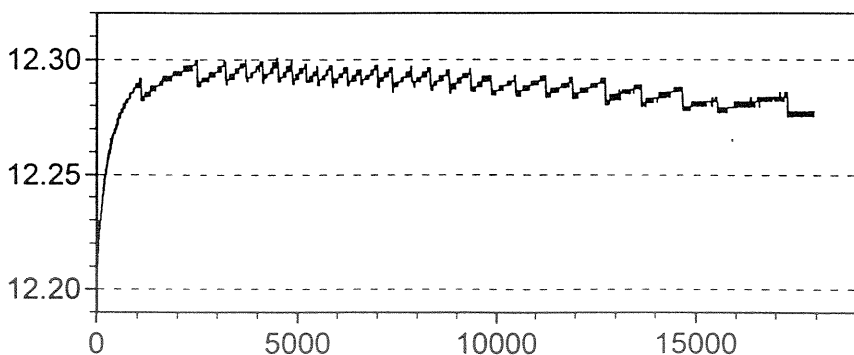
### Temperatursond 2

Placering Par. tunnel, vtn från värme-, temphål  
 Avstånd 0.154 m  
 Starttemperatur 12.67 °C  
 Värmeledningsförmåga 3.49 W/m°C  
 Värmediffusivitet 1.277E-06 m<sup>2</sup>/s  
 Värmekapacitet 0.76 kWh/m<sup>3</sup>°C  
 Standardavvikelse 0.000 °C



### Temperatursond 3

Placering Används inte  
 Avstånd 0.000 m  
 Starttemperatur 12.66 °C  
 Värmeledningsförmåga 0.00 W/m°C  
 Värmediffusivitet 0.000E+00 m<sup>2</sup>/s  
 Värmekapacitet 0.00 kWh/m<sup>3</sup>°C  
 Standardavvikelse 0.000 °C



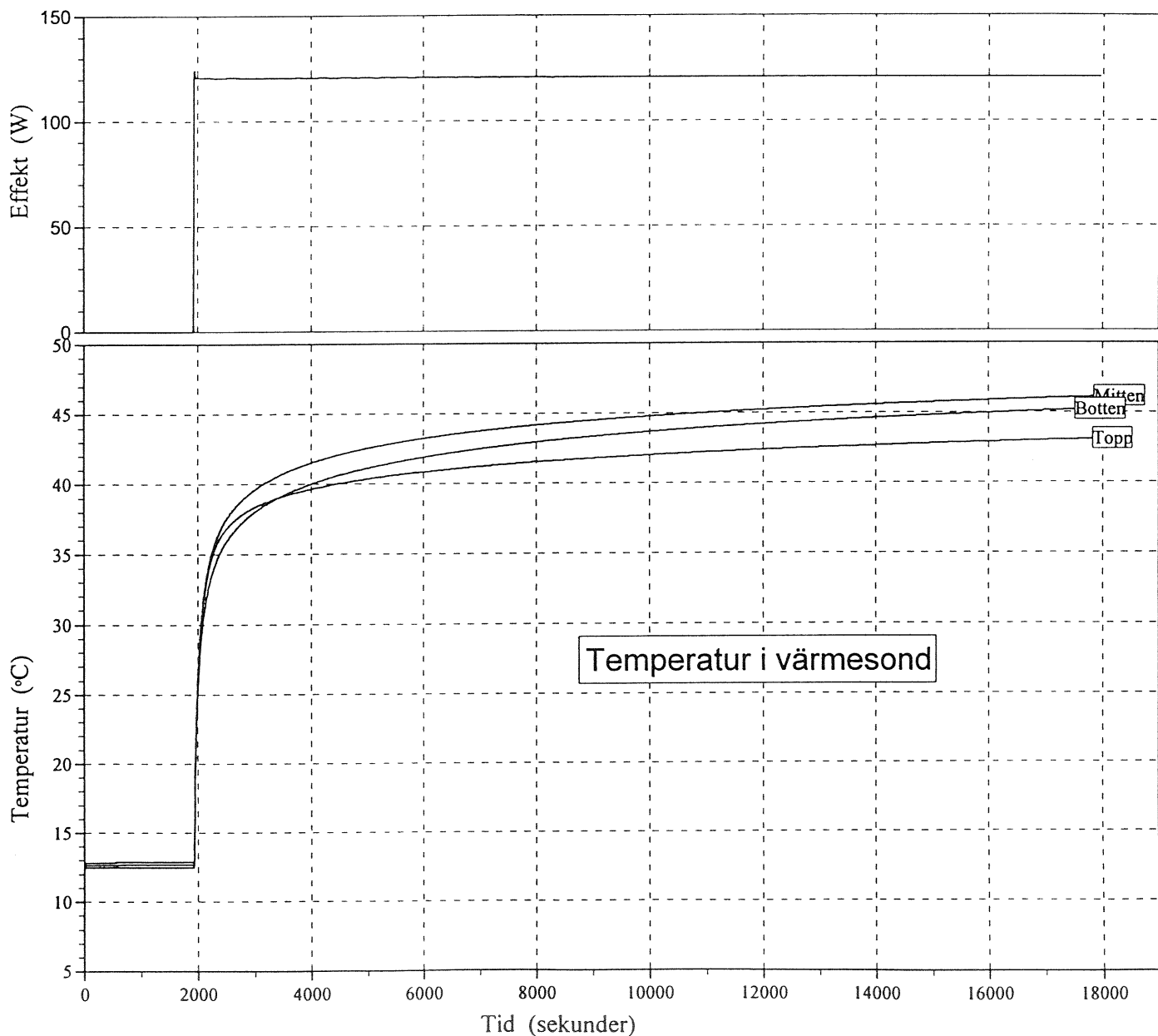
### Referenstemperatur

Placering Referenstemperatur  
 Avstånd 6.2 m  
 Medeltemperatur 12.29 °C  
 Standardavvikelse 0.0057 °C

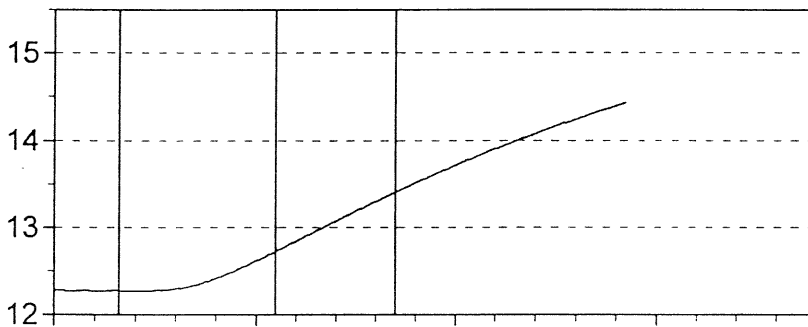
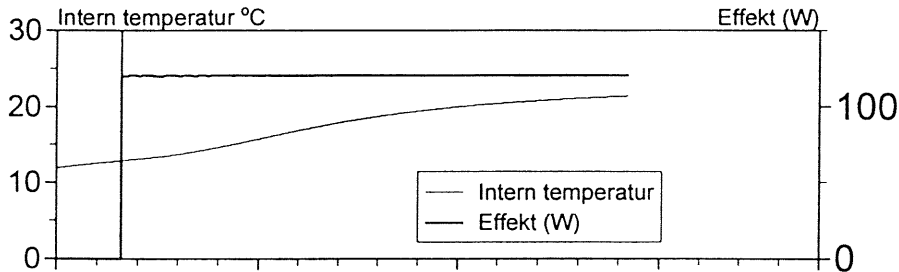
## ENERGI

## TERMISKA EGENSKAPER

Prototypförvaret - Äspö Tunnel, 450 m djup			Datum 1998-10-15	
			Projektnummer 2-9709-451	
Sektion 3535 höger (mätn.nr 1)	Provdjup 0,6 m	Material Homogen Äspödiorit		Signatur
Försöksdatum 98-01-21	Filnamn 3535-3C.TSW	Utfört av MB/AG		
Referenstemperatur 12.29 °C	Effekt 120.84 W 100.70 W/m	Beräkningsresultat		
Standardavvikelse 0.006 °C	Standardavvikelse 0.0204 W	Temperatursond 1	2	3
		Avstånd 0.149	0.154	0.000 m
		Värmeledningsförmåga 2.73	3.49	0.00 W/m°C
		Värmediffusivitet 1.27E-06	1.28E-06	0.00E+00 m²/s
		Värme kapacitet 0.60	0.76	0.00 kWh/m³°C

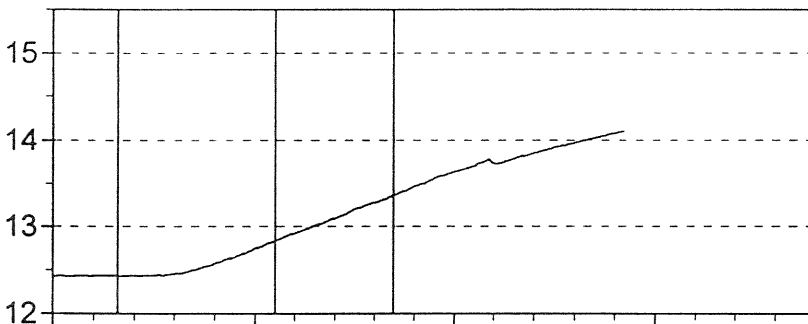


Projekt	Prototypförvaret - Äspö	Längd	1.20 m
Projektnummer	2-9709-451	Diameter	13 mm
Datum	98-01-27	Max effekt	120 W
Plats	Tunnel, 450 m djup	Max temperatur	100 grader
Sektion	3535 höger (mätn.nr2)	Värmspiralens resistans	7.2 ohm
Material	Homogen Äspödiorit	Värmspiralens längd	1200 mm
Provdjup	0,6 m		
Operatör	MB/AG		



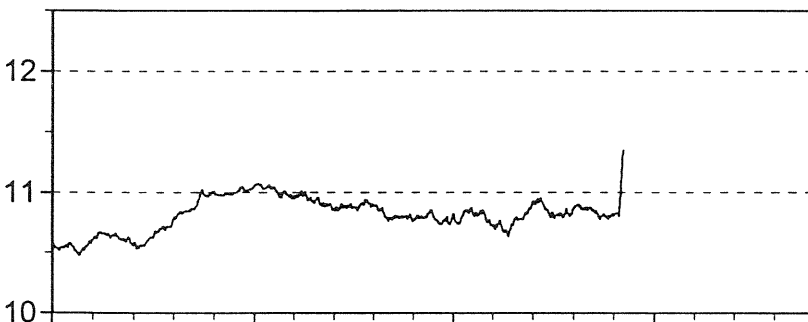
### Temperatursond 1

Placering V-rät tunnel, lite vatten fr värmehål  
 Avstånd 0.149 m  
 Starttemperatur 12.27 °C  
 Värmeledningsförmåga 2.67 W/m°C  
 Värmediffusivitet 1.167E-06 m²/s  
 Värmekapacitet 0.63 kWh/m³°C  
 Standardavvikelse 0.000 °C



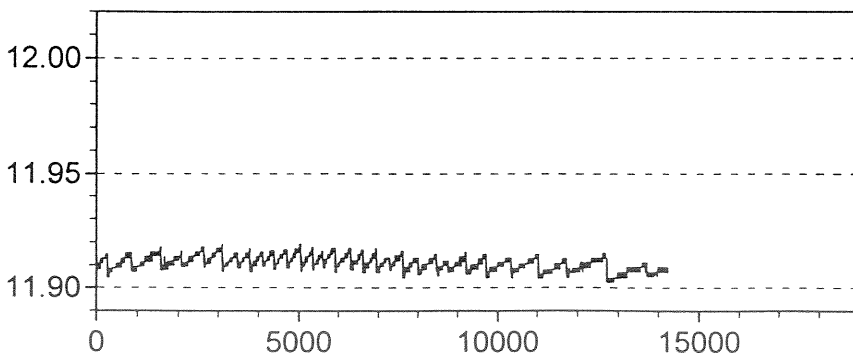
### Temperatursond 2

Placering Par. tunnel, vtn fr värme-, temphål  
 Avstånd 0.154 m  
 Starttemperatur 12.43 °C  
 Värmeledningsförmåga 3.76 W/m°C  
 Värmediffusivitet 1.390E-06 m²/s  
 Värmekapacitet 0.75 kWh/m³°C  
 Standardavvikelse 0.000 °C



### Temperatursond 3

Placering Används inte  
 Avstånd 0.000 m  
 Starttemperatur 10.58 °C  
 Värmeledningsförmåga 0.00 W/m°C  
 Värmediffusivitet 0.000E+00 m²/s  
 Värmekapacitet 0.00 kWh/m³°C  
 Standardavvikelse 0.000 °C



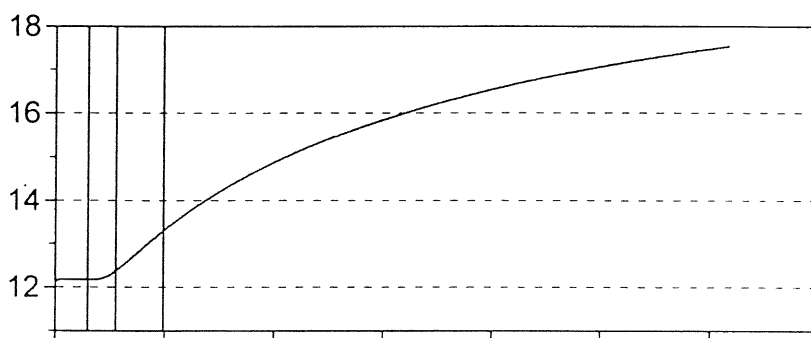
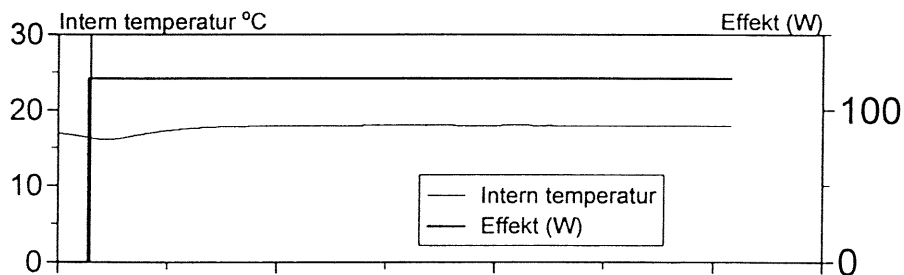
### Referenstemperatur

Placering Referenstemperatur  
 Avstånd 6.2 m  
 Medeltemperatur 11.91 °C  
 Standardavvikelse 0.0032 °C



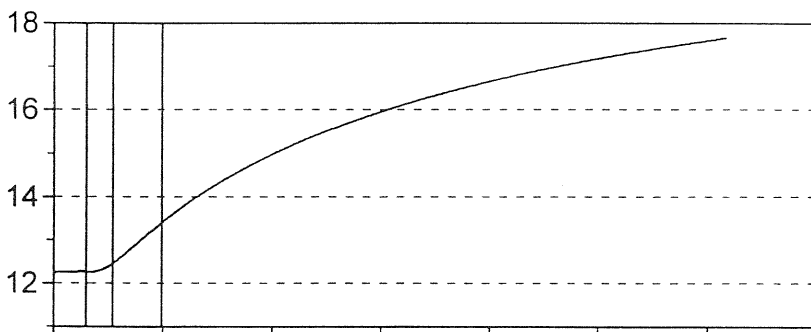


Projekt	Prototypförvaret - Äspö	Längd	1.20 m
Projektnummer	2-9709-451	Diameter	13 mm
Datum	98-01-28	Max effekt	120 W
Plats	Tunnel, 450 m djup	Max temperatur	100 grader
Sektion	3566 (höger )	Värmspiralens resistans	7.2 ohm
Material	Epidot samt homogen Äspödiorit	Värmspiralens längd	1200 mm
Provdjup	0,6 m		
Operatör	MB/AG		



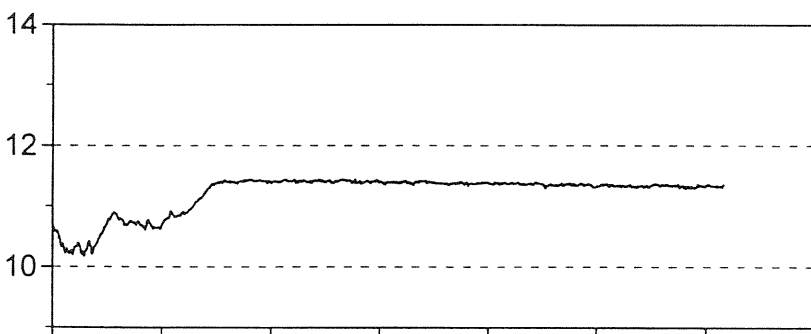
### Temperatursond 1

Placering	Äspödiorit
Avstånd	0.160 m
Starttemperatur	12.17 °C
Värmeledningsförmåga	3.16 W/m°C
Värmediffusivitet	1.509E-06 m <sup>2</sup> /s
Värmekapacitet	0.58 kWh/m <sup>3</sup> °C
Standardavvikelse	0.000 °C



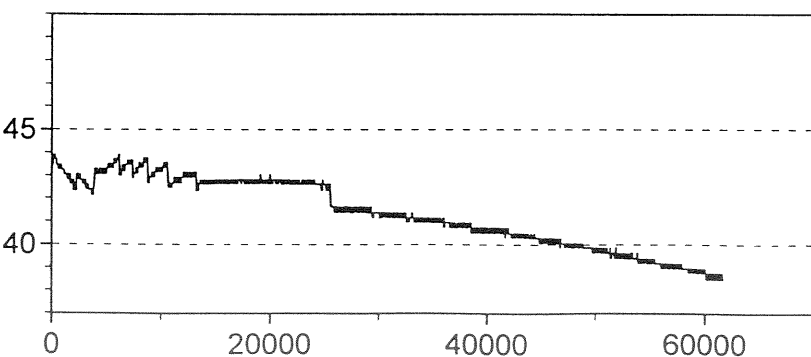
### Temperatursond 2

Placering	Över struktur
Avstånd	0.156 m
Starttemperatur	12.27 °C
Värmeledningsförmåga	3.19 W/m°C
Värmediffusivitet	1.449E-06 m <sup>2</sup> /s
Värmekapacitet	0.61 kWh/m <sup>3</sup> °C
Standardavvikelse	0.000 °C



### Temperatursond 3

Placering	Används inte
Avstånd	0.000 m
Starttemperatur	10.59 °C
Värmeledningsförmåga	0.00 W/m°C
Värmediffusivitet	0.000E+00 m <sup>2</sup> /s
Värmekapacitet	0.00 kWh/m <sup>3</sup> °C
Standardavvikelse	0.000 °C

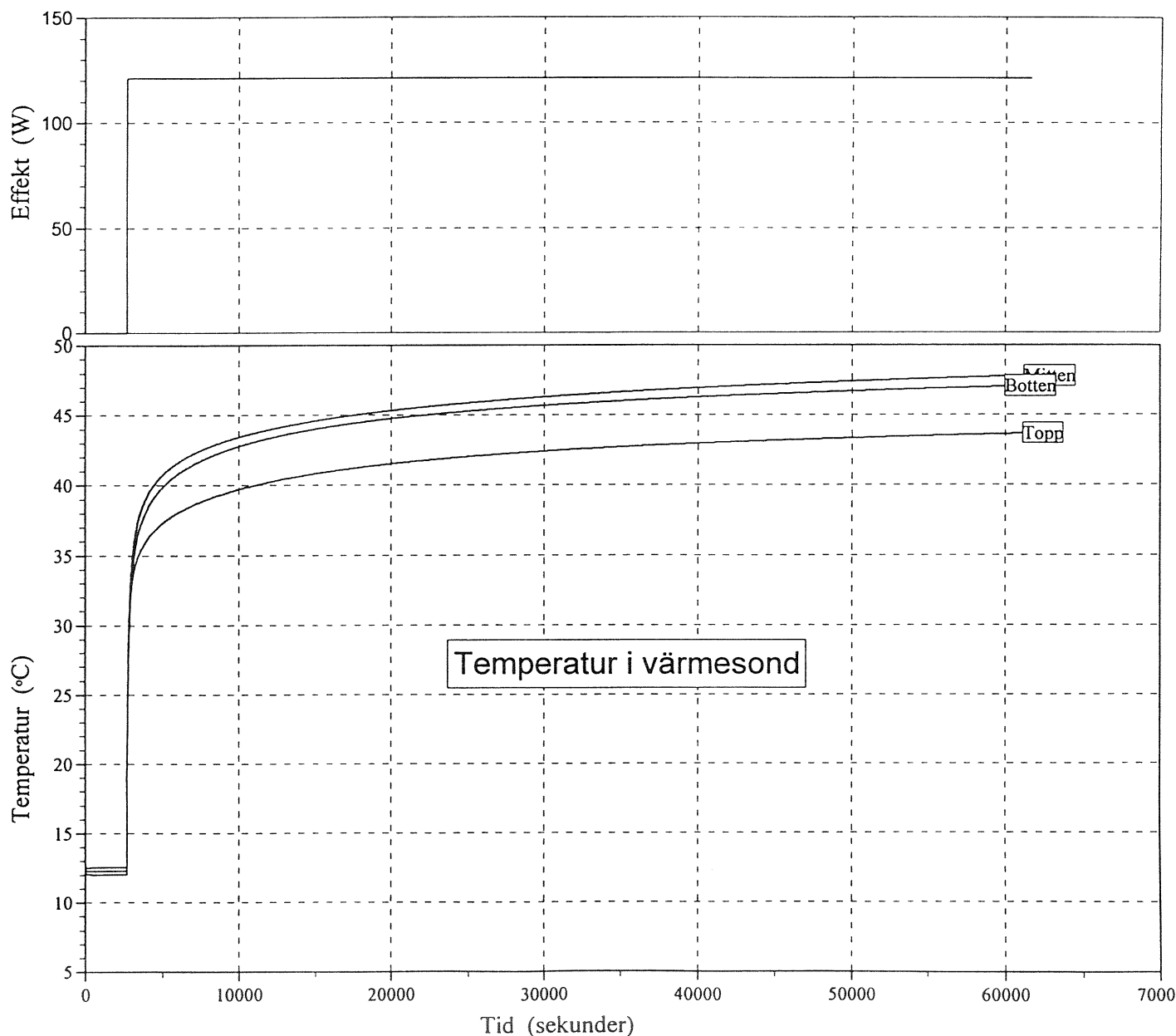


### Referenstemperatur

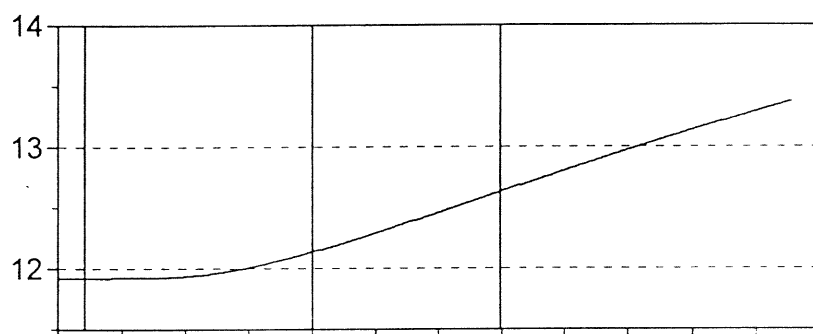
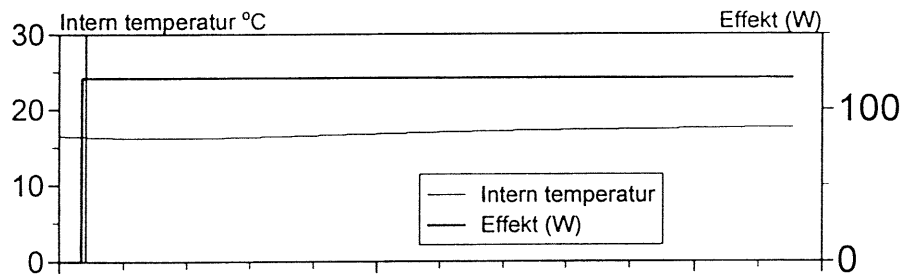
Placering	Referenstemperatur
Avstånd	7.5 m
Medeltemperatur	12.41 °C
Standardavvikelse	0.0147 °C

## TERMISKA EGENSKAPER

Prototypförväret - Äspö Tunnel, 450 m djup			Datum	1998-10-15	
			Projektnummer	2-9709-451	
Sektion	Provdjup	Material	Signatur		
3566 (höger)	0,6 m	Epidot samt homogen Äspödiorit			
Försöksdatum	Filnamn	Utfört av			
98-01-28	3566-6A.TSW	MB/AG			
Referenstemperatur	Effekt	Beräkningsresultat			
12.41 °C	121.19 W 100.99 W/m	Temperatursond	1	2	3
Standardavvikelse	Standardavvikelse	Avstånd	0.160	0.156	0.000 m
0.015 °C	0.0166 W	Värmeledningsförmåga	3.16	3.19	0.00 W/m°C
		Värmediffusivitet	1.51E-06	1.45E-06	0.00E+00 m <sup>2</sup> /s
		Värmekapacitet	0.58	0.61	0.00 kWh/m <sup>3</sup> °C

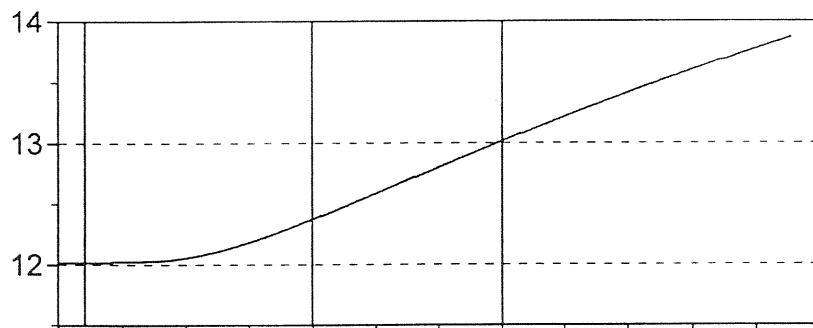


Projekt	Prototypförvaret - Äspö	Längd	1.20 m
Projektnummer	2-9709-451	Diameter	13 mm
Datum	98-01-28	Max effekt	120 W
Plats	Tunnel, 450 m djup	Max temperatur	100 grader
Sektion	3583	Värmespiralens resistans	7.2 ohm
Material	Homogen Äspödiorit	Värmespiralens längd	1200 mm
Provdjup	0,6 m		
Operatör	MB/AG		



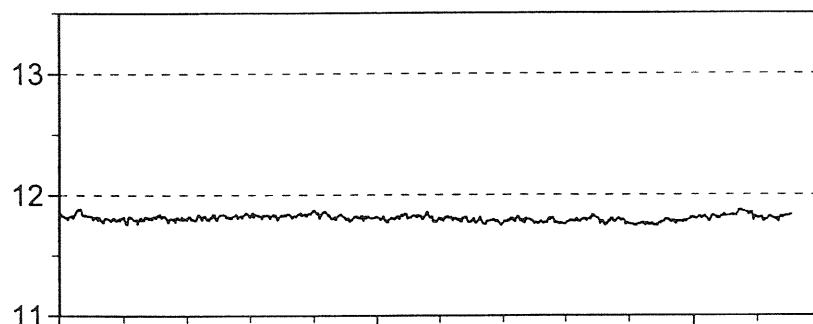
### Temperatursond 1

Placering	Homogen Äspödiorit
Avstånd	0.168 m
Starttemperatur	11.92 °C
Värmeledningsförmåga	2.80 W/m°C
Värmediffusivitet	1.159E-06 m <sup>2</sup> /s
Värmekapacitet	0.67 kWh/m <sup>3</sup> °C
Standardavvikelse	0.000 °C



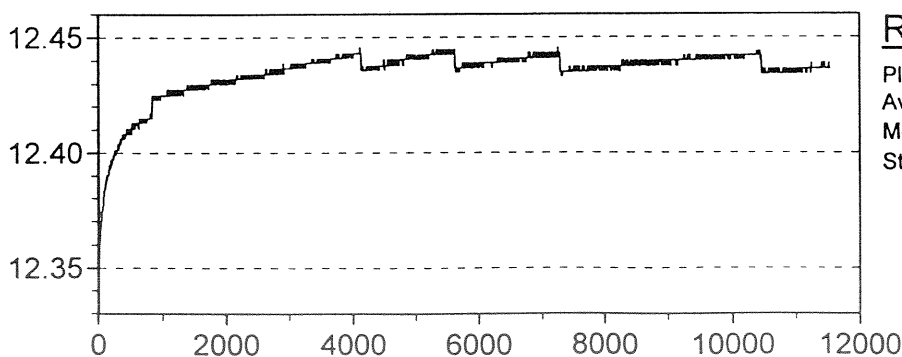
### Temperatursond 2

Placering	Homogen Äspödiorit
Avstånd	0.159 m
Starttemperatur	12.02 °C
Värmeledningsförmåga	2.78 W/m°C
Värmediffusivitet	1.293E-06 m <sup>2</sup> /s
Värmekapacitet	0.60 kWh/m <sup>3</sup> °C
Standardavvikelse	0.000 °C



### Temperatursond 3

Placering	Används inte
Avstånd	0.000 m
Starttemperatur	11.80 °C
Värmeledningsförmåga	0.00 W/m°C
Värmediffusivitet	0.000E+00 m <sup>2</sup> /s
Värmekapacitet	0.00 kWh/m <sup>3</sup> °C
Standardavvikelse	0.000 °C



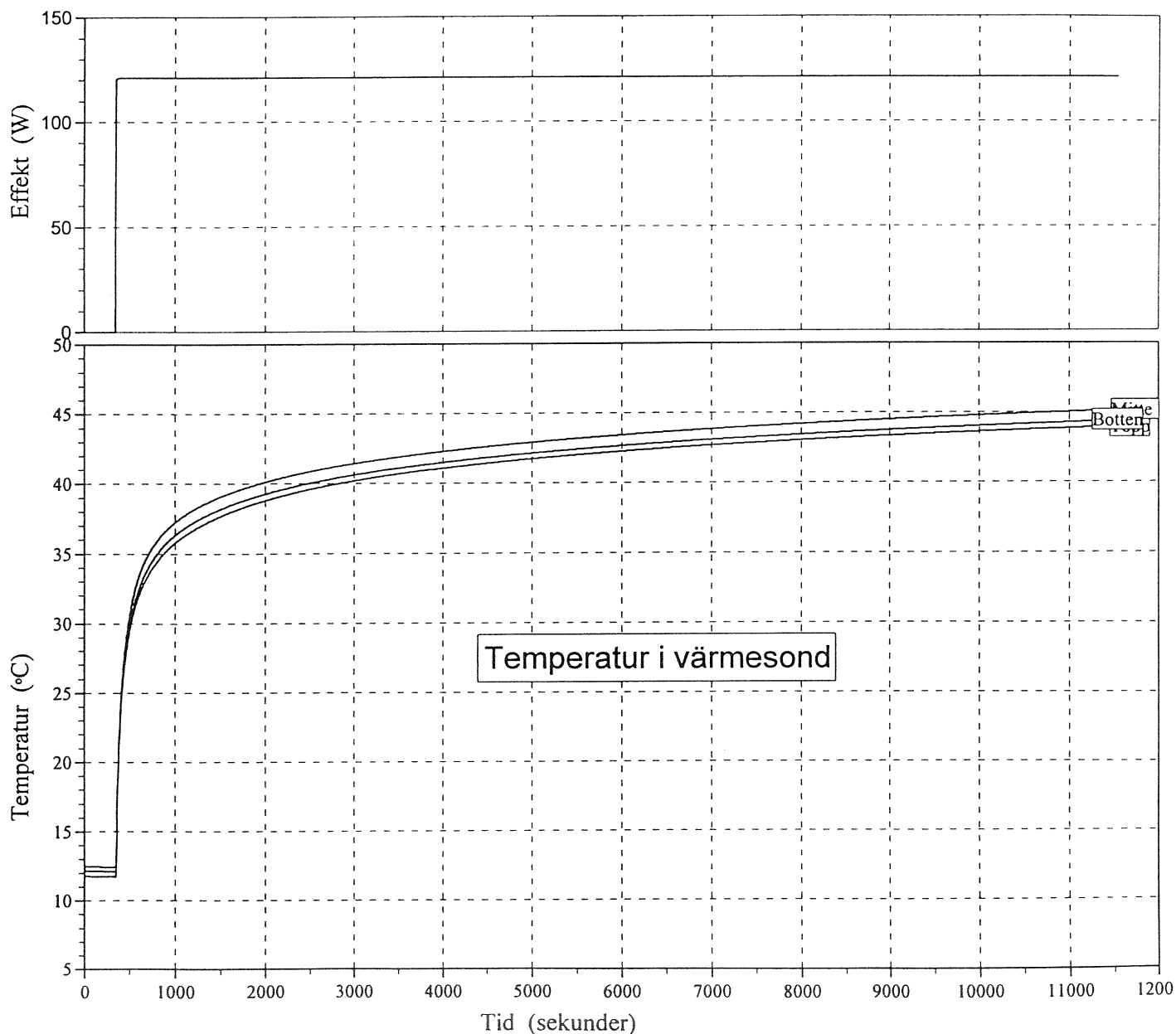
### Referenstemperatur

Placering	Referenstemperatur
Avstånd	9.1 m
Medeltemperatur	12.44 °C
Standardavvikelse	0.0065 °C

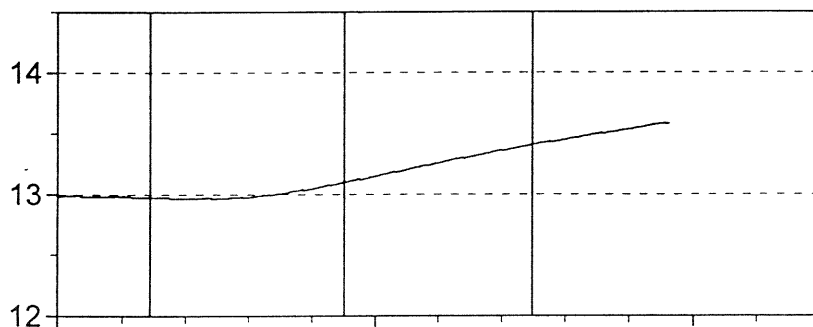
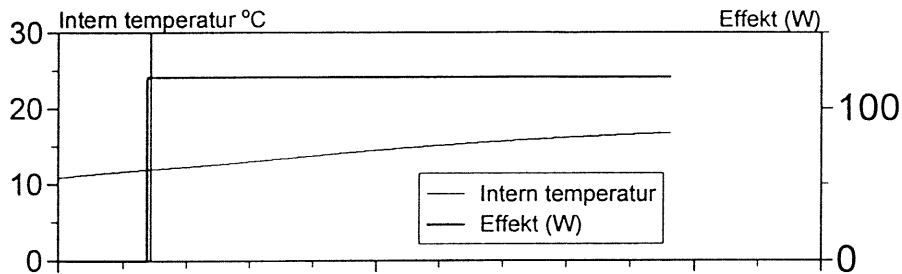
## ENERGI

## TERMISKA EGENSKAPER

Prototypförväret - Äspö Tunnel, 450 m djup			Datum 1998-10-15		
			Projektnummer 2-9709-451		
Sektion 3583	Provdjup 0,6 m	Material Homogen Äspödiorit		Signatur	
Försöksdatum 98-01-28	Filnamn 3583-2A.TSW	Utfört av MB/AG			
Referenstemperatur 12.44 °C	Effekt 121.23 W 101.03 W/m	Beräkningsresultat			
Standardavvikelse 0.007 °C	Standardavvikelse 0.0293 W	Temperatursond	1	2	3
		Avstånd	0.168	0.159	0.000 m
		Värmeledningsförmåga	2.80	2.78	0.00 W/m°C
		Värmediffusivitet	1.16E-06	1.29E-06	0.00E+00 m²/s
		Värmekapacitet	0.67	0.60	0.00 kWh/m³°C

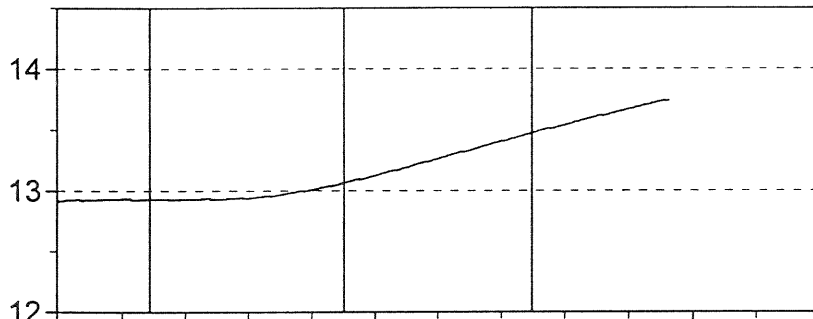


Projekt	Prototypförvaret - Äspö	Längd	1.20 m
Projektnummer	2-9709-451	Diameter	13 mm
Datum	98-01-28	Max effekt	120 W
Plats	Tunnel, 450 m djup	Max temperatur	100 grader
Sektion	3594 vänster	Värmspiralens resistans	7.2 ohm
Material	Struktur+diorit. Vtntryck övre delen	Värmspiralens längd	1200 mm
Provdjup	0,6 m		
Operatör	MB/AG		



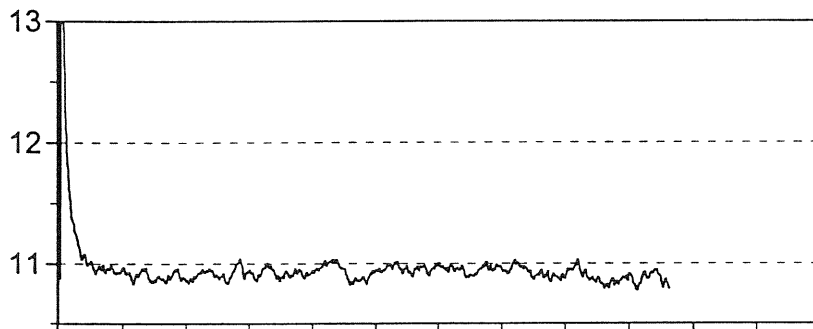
### Temperatursond 1

Placering Diorit, spricka m hål, vtn båda håler  
 Avstånd 0.165 m  
 Starttemperatur 12.98 °C  
 Värmeledningsförmåga 5.98 W/m°C  
 Värmediffusivitet 1.451E-06 m<sup>2</sup>/s  
 Värmekapacitet 1.14 kWh/m<sup>3</sup>°C  
 Standardavvikelse 0.000 °C



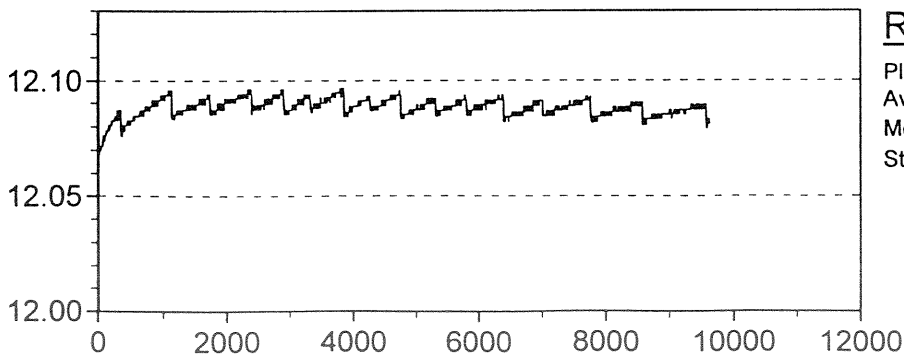
### Temperatursond 2

Placering Struktur, vatten fr värnehålet  
 Avstånd 0.166 m  
 Starttemperatur 12.93 °C  
 Värmeledningsförmåga 3.64 W/m°C  
 Värmediffusivitet 1.228E-06 m<sup>2</sup>/s  
 Värmekapacitet 0.82 kWh/m<sup>3</sup>°C  
 Standardavvikelse 0.000 °C



### Temperatursond 3

Placering Används inte  
 Avstånd 0.000 m  
 Starttemperatur 10.90 °C  
 Värmeledningsförmåga 0.00 W/m°C  
 Värmediffusivitet 0.000E+00 m<sup>2</sup>/s  
 Värmekapacitet 0.00 kWh/m<sup>3</sup>°C  
 Standardavvikelse 0.000 °C



### Referenstemperatur

Placering Referenstemperatur  
 Avstånd 20.4 m  
 Medeltemperatur 12.09 °C  
 Standardavvikelse 0.0031 °C

## ENERGI

## TERMISKA EGENSKAPER

Prototypförvaret - Äspö Tunnel, 450 m djup			Datum	1998-10-15	
			Projektnummer	2-9709-451	
Sektion	Provdjup	Material	Signatur		
3594 vänster	0,6 m	Struktur+diorit. Vtntryck övre delen			
Försöksdatum	Filnamn	Utfört av			
98-01-28	3594-1A.TSW	MB/AG			
Referenstemperatur	Effekt	Beräkningsresultat			
12.09 °C	120.72 W 100.60 W/m	Temperatursond	1	2	3
Standardavvikelse	Standardavvikelse	Avstånd	0.165	0.166	0.000 m
0.003 °C	0.0185 W	Värmeledningsförmåga	5.98	3.64	0.00 W/m°C
		Värmediffusivitet	1.45E-06	1.23E-06	0.00E+00 m <sup>2</sup> /s
		Värmekapacitet	1.14	0.82	0.00 kWh/m <sup>3</sup> °C

